Generation of Helical States - Breaking of Symmetries, Curie's Principle, and Excited States

Julia Sabalot-Cuzzubbo, W Lafargue-Dit-Hauret, Michel Rérat, K Costuas, Didier Bégué, Jacky Cresson

10.1002/cphc.202200951
WILEY-VCH

Generation of Helical States - Breaking of Symmetries, Curie's Principle, and Excited States

Julia Sabalot-Cuzzubbo,[a] William Lafargue-Dit-Hauret,[+,a] Michel Rérat,[+,a] Karine Costuas,[+,b] Didier Bégué,*[a] Jacky Cresson,*[c]

Herein, we deeply detail for the very first time mathematical concepts behind the generation of helical molecular orbitals (MOs) for linear chains of atoms. We first give a definition of helical MOs and we provide an index measuring how far a given helical states is from a perfect helical distribution. Structural properties of helical distribution for twisted $[N]$-cumulene and cumulene version of Möbius systems are given. We then give some simple structural assumptions as well as symmetry requirements ensuring the existence of helical MOs. Considering molecules which do not admit helical MOs, we provide a first way to induce helical states by the breaking of symmetries. We also explore an alternative way using excited conformations of given molecules as well as different electronic multiplicities.

Introduction

During the past few years, a huge interest has been developed for particular linear chains of atoms like cumulene or carbyne. One of the interests is to possess in some configurations, helical MOs along the chain opening new possibilities in nanoscale electronics[1–10]. This phenomenon called **electrohelicity** has been discussed in several different ways, in particular, using classical Hückel theory and symmetry group (see for example Ref. 1) or from a more physical point of view using properties of the Hamiltonian (see for example Ref. 11). To our knowledge, these works are restricted to molecules in their ground state and no studies provide a discussion of the effect of excited states[12] as well as electronic multiplicities on electrohelicity.

First, we define helical MOs following the previous work of M. H. Garner et al.[1] and S. Gunasekaran et al.[11]. A helical MO is associated to a given distribution of vectors or angles associated to the π-system. The classical picture is to draw a helix representing the twist of the π-vectors along the structure. In Ref. 10, W. Bro-Jørgensen et al. study how far a given distribution is from a perfect helix, *i.e.* a distribution governed by a fixed pitch. We introduce an index based on the standard least square method giving the best perfect helix fitting to a given helical distribution. We take this opportunity to give general results about Hückel distributions of twisted $[N]$-cumulene and equivalent cumulene version of Möbius systems.

Second, we review previous work leading to a characterization of electrohelicity in term of basic structural assumptions on the linear chain and symmetry properties[13]. This characterization can be used to precisely identify which kind of atoms can be used to construct molecule admitting electrohelicity. Chirality plays an important role in this setting and is supported by a general physical argument called the Curie's principle.

Third, taking molecules which do not support electrohelicity in their ground state, we explain how to obtain it by looking to excited states or electronic multiplicities. Such a possibility is only valid for molecules which in their ground state admit a subgroup with the basic ingredients of electrohelicity. In this case, using symmetry adapted MOs, we are able to predict the properties of the induced helical MOs.

Finally, we illustrate our discussion with several examples.

Results and Discussion

Helical States and some Properties

Definition of Helical States

In this section, we are guided by the work of S. Gunasekaran et al.[11]. We consider a chain of $N-1$ sp-atoms A_i denoted by C, together with arbitrary left and right end groups denoted by L and R, consisting of a connection with an sp^2-atom with a given structure (see Figure 1). The chain C of atoms is oriented along the z-axis. The π-system of the chain can be modelled with a basis set comprising a p_x and p_y orbital for each atom of the chain. The p_z-orbital is directed along the chain direction and is part of the σ-system.

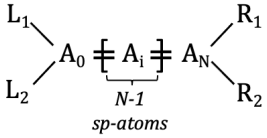

Figure 1. Representation of a standard chain

The left and right groups can have arbitrary shapes, but the most usual situation encountered for this type of chain-compound is that of unsubstituted methylene (alkylidene) like cumulenes where $L_1 =$

[a] Dr. J. Sabalot-Cuzzubbo, Dr. W. Lafargue-Dit-Hauret, Prof. Dr. M. Rérat, Prof. Dr. D. Bégué*
Universite de Pau et des Pays de l'Adour, E2S UPPA, CNRS, IPREM, Pau, France
E-mail: didier.begue@univ-pau.fr

[b] Dr. K. Costuas
Université Rennes, CNRS, ISCR (Institut des Sciences Chimiques de Rennes) - UMR 6226, F-35000 Rennes, France

[c] Prof. Dr. J. Cresson
Universite de Pau et des Pays de l'Adour, E2S UPPA, CNRS, LMAP, Pau, France
E-mail: jacky.cresson@univ-pau.fr

[+] These authors contributed equally.

10.1002/cphc.202200951
WILEY-VCH

$L_2 = H$ and $R_1 = R_2 = H$. The cumulene molecule with N double bonds is denoted as $[N]$-cumulene. In their ground-states cumulenes with even numbers of carbon atoms and hence with odd numbers of double bonds are planar (eclipsed conformation). Cumulenes with odd numbers of carbon atoms are nonplanar, with orthogonal planes of the terminal methyl groups.

Our interest is on the **orbital structure** restricted to the chain C, meaning that we will not discuss the particular orbital structure emerging in the left and right side groups. Also, we focus on **helical orbitals** which were discussed by M. H. Garner and co-workers in Ref. 1 in connection with cumulenes and annulenes. Helical orbitals allow a π-electron delocalization twisting along the chain.

Formally, this can be viewed as follows. Let E be a given energy and z the integer position of the atoms of the chain with $z = 0$ corresponding to the left side and $z = N$ to the right side. Denoted by $\psi(z)$ the atomic molecular orbital associated to atoms $A(z)$, we have Eq. 1:

$$\psi(z) = \begin{pmatrix} \psi_x(z) \\ \psi_y(z) \end{pmatrix} = MR(z\omega)v_0 \tag{1}$$

where v_0 is a fixed two-dimensional unit vector, $\omega \in \mathbb{R}$, $R(z\omega)$ is the rotation matrix of angle $z\omega$ and M is a real symmetric matrix.

As the vector $R(z\omega)v_0$ belongs to the unit circle S^1, the vector $\psi(z)$ belongs to the image of the unit circle by the linear map associated to M. Denoted by v_a and v_b the two orthogonal eigenvectors of M associated to the eigenvalues a and b which are real, the image of S^1 is an ellipse whose major/minor axis are given by av_a and bv_b. The vector $\psi(z)$ rotates along the ellipse when z increases. The orientation of the rotation when z increases depends on M, which characterizes the elliptic polarization. If $|M| > 0$ (resp. $|M| < 0$) the rotation is clockwise (resp. counterclockwise).

Fitting a Helix to Helical MOs

We first introduce the notion of distribution of angles. We call the **distribution associated to** ψ and we denote by $\mathscr{D}(\psi)$ a finite family of angles $\phi(z_j)$, $j = 0, \ldots, m$ or equivalently a finite family of unit vectors $\psi(z_j) \in S^1$, where $z_j \in \mathbb{R}$ is an increasing family of real values.

Remark 1. *It must be noted that in principle a helical MO induces a continuous distribution of angles $\phi(z)$ but in practice we will have access only to a sampling of this distribution.*

We can represent a distribution by sections along a cylinder oriented along the z-axis. A linear molecule being given, a distribution can be obtained in essentially two different ways:

- First, we can use Hückel theory in order to determine an approximation of the wave function along the molecule, and a vector $\psi(z)$ corresponding to the decomposition of it in the basis given by $p_x(z)$ and $p_y(z)$ at the atom positioned at point z. Such a distribution will be denoted by $\mathscr{D}_{Huckel}$.
- We can use DFT in order to determine the vector $\psi(z)$ using the technique developed by W. Bro-Jørgensen et al. in Ref. 10. Such a distribution will be denoted by $\mathscr{D}_{DFT}$.

Remark 2. *The previous distributions are not the only ones which can be defined. Observations deduced from DFT are sometimes subject to caution. As a consequence, one can imagine using more refined methods for example CASSCF (Complete Active Space) in order to check if the underlying phenomenon is method's dependent or not (see Supporting Information). In the following, we then also studied $\mathscr{D}_{CASSCF}$.*

We can associate to each distribution $\mathscr{D}(\psi)$ a continuous helix in the following sense. For each set of real constants $b > 0$, $\gamma \in \mathbb{R}$, $\varepsilon = \pm 1$ and $r > 0$ (an example is provided in Figure 2), one can defined an helix $h_{r,b,\varepsilon}$ whose parametrization is given by Eq. 2:

$$\begin{cases} x(t) &= r\cos(\gamma t), \\ y(t) &= \varepsilon r \sin(\gamma t), \\ z(t) &= b\gamma t. \end{cases} \tag{2}$$

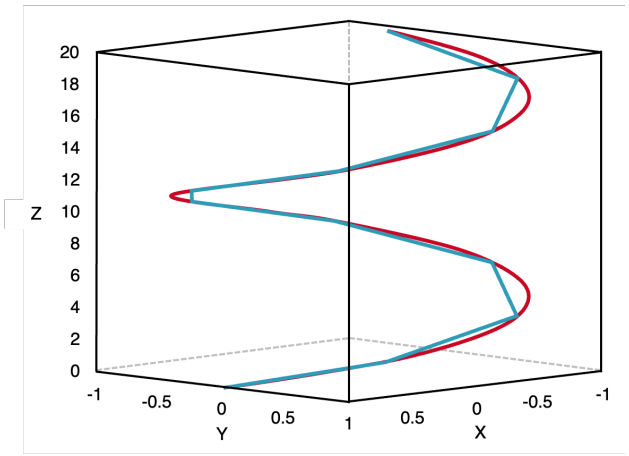

Figure 2. Perfect helix curve based on Eq. 2 with $b = 2$, $r = 1$, $\gamma = 1$, $\varepsilon = 1$.

Another way to write the parametrization is provided in Eq. 3:

$$h_{r,b,\gamma,\varepsilon}(t) = r\left(\cos(\gamma t)e_x + \varepsilon \sin(\gamma t)e_y\right) + b\gamma t e_z, \tag{3}$$

where (e_x, e_y, e_z) is the canonical basis defined by $e_x = (1,0,0)$, $e_y = (0,1,0)$, $e_z = (0,0,1)$.

In the following, we simply denote $h_{b,\gamma,\varepsilon}$ for $h_{r,b,\gamma,\varepsilon}$. If the parameter $\varepsilon = 1$ (resp. -1), then the helix is right-hand (resp. left-hand). For each distribution $\mathscr{D}(\psi)$ one can look for the best helix $h_{b,\varepsilon}$ which minimizes the quantity in Eq. 4:

$$L(r,b,\gamma,\varepsilon) = \sum_{i=0}^{m} \| \psi(z_i) - h_{r,b,\gamma,\varepsilon}(z_i) \|^2 \tag{4}$$

The sign of ε for a given distribution is easy to determine, so that we are reduced to the minimization of the functional in Eq. 5:

$$L(r,b,\gamma) = \sum_{i=0}^{m} \| \psi(i) - h_{r,b,\gamma,\varepsilon}(i) \|^2, \tag{5}$$

where ε is fixed.

Such a problem is solved using the **non linear least squares method**. In general **no unique solution is found** and **no explicit formula** can be given from the data because the method is an iterative process. Another possibility is to restrict our attention to the distribution angles instead of the specific geometry of the helix. This is done in the next section.

Fitting a Helical Distribution - Cumulated Angle

Helix with a constant pitch b induces a distribution of the form of Eq. 6:

$$\mathscr{D}_{Helix} = \{\phi(z_i) = z_i/b,\ i = 0, \ldots, N\} \tag{6}$$

As a consequence, if one considers the **cumulated angle** defined by Eq. 7:

$$\phi_c(i) = \sum_{1}^{i} |\ \phi(z_j) - \phi(z_{j-1})\ | \quad \text{with} \quad \phi_c(z_0) = 0, \tag{7}$$

10.1002/cphc.202200951
WILEY-VCH

one obtains Eq. 8:

$$\phi_c(z) = \frac{1}{b}z, \tag{8}$$

i.e. a straight line passing through 0 with a constant slope $1/b$. An idea is then to compare the set of points $(z_j, \phi_c(z_j))$, $j = 0;\ldots,N$ of a given helical distribution with a set of helical points $(z_j, z_j/b)$, by minimizing the quantity in Eq. 9:

$$\mathscr{L}(b) = \sum_{i=0}^{n} \left(\phi_c(j) - f_j\right)^2, \tag{9}$$

where $f_j = z_j/b$, *i.e.* to use the (linear) **least squares method** or **regression analysis** in order to obtain the best fitted **straight line** of the form of Eq. 10:

$$\phi = \alpha\,(z - z_0) + \phi_0, \tag{10}$$

where $\alpha \in \mathbb{R}$ has to be determined, to the set of data $\phi_c(z_j)$. It must be noted that the special form of the straight line is due to the fact that we impose on the line to pass through the initial point $(z_0, \phi_c(0)$ which is the first value of the cumulated angles distribution.

As we usually choose $z_0 = 0$ for the position of the first atom and $\phi_c(0)) = 0$, the optimization problem reduces to find the best linear line expressed in Eq. 11:

$$\phi = \alpha z \tag{11}$$

which fits the set of data $\phi_c(z_j)$.

Remark 3. *A similar idea is used by W. Bro-Jørgensen et al.*[10], *where the authors define the* ***MAD index*** *which corresponds to the* ***mean of the absolute deviation*** $\mid \phi_c(z_j) - f_j \mid$.

The solution to the previous problem has an explicit analytical solution given by Eq. 12:

$$\alpha = \frac{\sigma(\phi_c(z), z) + \overline{\phi_c(z)}\bar{z}}{\sigma^2(z)}, \tag{12}$$

where for two given series $x = (x_0,\ldots,x_N)$, $y = (y_0\ldots,y_N)$, we denote by Eqs. 13 to 15:

$$\bar{x} = \frac{1}{N+1}\sum_{i=0}^{N} x_i, \tag{13}$$

$$\sigma(x,y) = \sum_{i=0}^{N} \frac{(x_i - \bar{x})(y_i - \bar{y})}{N+1}, \tag{14}$$

$$\sigma^2(x) = \sum_{i=0}^{N} \frac{(x_i - \bar{x})^2}{N+1}, \tag{15}$$

the mean of x, covariance between x and y and variance of x. Let us denote by $\rho(x,y)$ the **correlation** factor defined by Eq. 16:

$$\rho(x,y) = \frac{\sigma(x,y)}{\sigma(x)\sigma(y)} \tag{16}$$

The quality of the approximation given by the regression line is measured by $\rho(\phi_c(z), z)$. If $\rho^2(\phi_c(z), z)$ is very close to one then the approximation is very good.

Remark 4. *As usual, the quality of the indicator is related to the quality of measure and it is subject to discussion. In general, for very good, measured quantities, a correlation* > 0.95 *is assumed to represent a very good approximation by a straight line.*

Consequently, we propose as an indicator of helicity the quantity in Eq. 17:

$$HEL = \rho(\phi_c(z), z), \tag{17}$$

instead of the MAD index proposed in Ref. 10. Two advantages at least can be pointed out:

- First, the correlation quantity is well-known and its interpretation, even if it is subject to discussion, is well documented.
- Second, a comparison is possible as $HEL \in [0,1]$. Contrarily, the MAD index can take arbitrary values and it is not clear what is the exact difference between a MAD index of 4, 7 or 10 as no normalization is given.

As an example, let us take the following angle distributions obtained for equivalent [4]-cumulene version of Möbius systems (see Properties of Distributions for $\boldsymbol{C_2}$-Adapted MOs of $\boldsymbol{\theta = 0}$ or $\boldsymbol{\theta = \frac{\pi}{2}}$ Twisted Cumulene) when $n = 1$ given by Eq. 18:

$$\mathscr{D}_{4,1} = \{0, 32, 45, 58, 90\} \tag{18}$$

The associated cumulated distribution is given by Eq. 19:

$$\phi_c = \{0, 32, 77, 135, 225\} \tag{19}$$

The "best" perfect helix fitting this set of data is given by Eq. 20:

$$\phi(z) = 49.7z, \tag{20}$$

and the correlation factor is given by Eq. 21:

$$\rho(z, \phi_c(z)) = 0.9887211, \tag{21}$$

which shows very good agreement (see Figure 3).

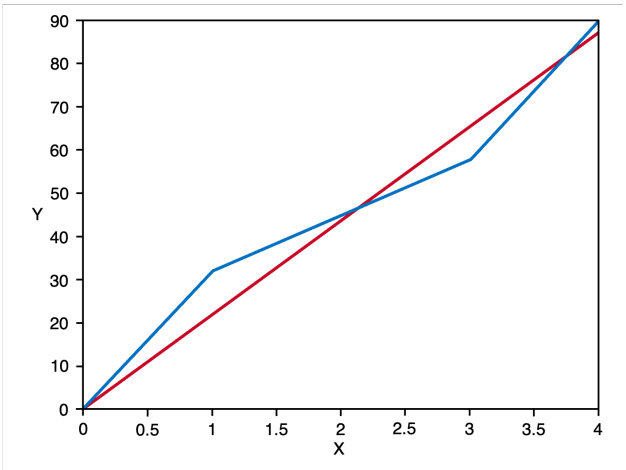

Figure 3. Best fitted helix for distribution of equivalent [4]-cumulene version of a Möbius system and $n = 1$.

The same can be done for the distribution of the equivalent [4]-cumulene version of a Möbius system when $n = 2$. In this case, the distribution is given by Eq. 22:

$$\mathscr{D}_{4,1} = \{0, 58, 135, 212, 270\}\,. \tag{22}$$

The associated cumulated distribution is given by Eq. 23:

$$\phi_c = \{0, 58, 193, 405, 675\}\,. \tag{23}$$

The "best" perfect helix fitting this set of data is given by Eq. 24:

$$\phi(z) = 145.3z, \tag{24}$$

and the correlation factor is given by Eq. 25:

$$\rho(z, \phi_c(z)) = 0.9794173, \tag{25}$$

which again this shows a very good fit (see Figure 4). Taking the solution of the minimisation problem, we can represent the π-system along the C system like a helix as depicted in Figure 5.

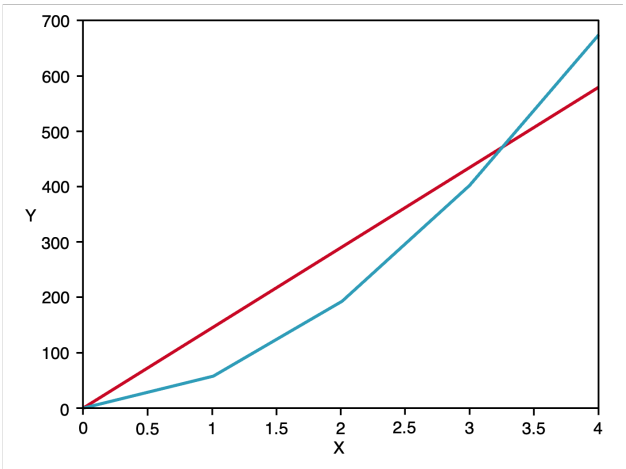

Figure 4. Best fitted helix for distribution of equivalent [4]-cumulene version of a Möbius system and $n = 2$

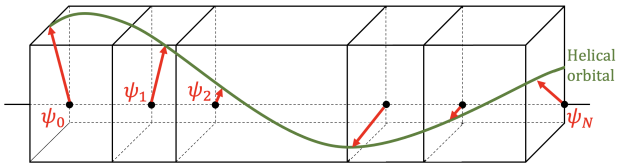

Figure 5. Representation of the π-system along the C system

Fitting a Helix - General Case

Classical helixes are called **perfect helixes** in Ref. 10. However, perfect helixes are not the rule as many examples already proven (see the next sections and Ref. 1). A more general class of helix is given by helix with a non-constant pitch, *i.e.* a helix of the form of Eq. 26:

$$\begin{cases} x(t) &= r\cos(t), \\ y(t) &= \varepsilon r\sin(t), \\ z(t) &= P(t), \end{cases} \tag{26}$$

where $P(t)$ is a smooth increasing function (see Figure 6).

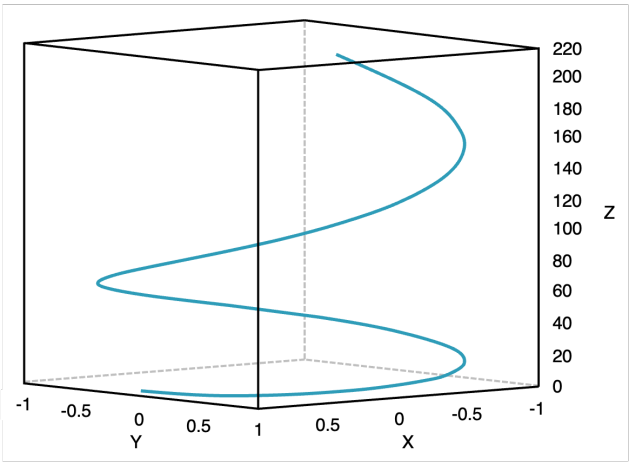

Figure 6. Imperfect helix based on Eq. 26 with $P(t) = 2t^2 + 3$.

More generally, one can consider a helix with a non-constant radius of the form of Eq. 27:

$$\begin{cases} x(t) &= r(t)\cos(t), \\ y(t) &= \varepsilon r(t)\sin(t), \\ z(t) &= P(t), \end{cases} \tag{27}$$

where $r : \mathbb{R} \mapsto \mathbb{R}^+$ is an arbitrary positive function.

A very good approximation of the function P can be obtained from the set of data completing the best helix approximation just studied but in a nonlinear setting, for example using polynomial functions for $P(t)$ as well as for $r(t)$. The previous generalization is not only a mathematical idea as shown in Figure 7 which evidences the general helix structure of a linear molecule.

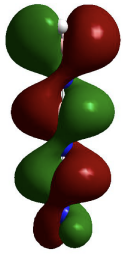

Figure 7. Non standard helix

In fact, a very large class of morphology is possible, and the case of perfect helix seems to be not representative of helical state. In that respect, it seems unreasonable to take a perfect helix as a structure to make comparisons with. Linear chains of boron nitride[14] could illustrate the existence of non standard helix. Like carbon nanostructures, boron nitride (BN) nanostructures present a wide variety of physical and chemical properties. They also present a wide variety of MOs according to both the number of atoms on the chains (even or odd), and to the nature of the A_0 and A_N atoms (boron or nitrogen) as illustrated in Figure 8 and in Supporting Information (Tables S3 and S4).

Some Properties of Hückel Distributions for $0 < \theta < \frac{\pi}{2}$ Twisted [N]-Cumulene

From a theoretical point of view, helical Hückel distributions are the only ones that can be dealt with. A complete treatment can be done for twisted $[N]$-cumulene. In this case the Hückel distribution $\mathscr{D}_{Huckel}(\theta)$ is obtained through the set of vectors given by Eq. 28:

$$\psi_n(z) = a_n R\left(\frac{\theta}{2}\right) D_{\frac{b_n}{a_n}} R(k_n z + \delta_n), \tag{28}$$

where $D_\lambda : \mathbb{R}^2 \mapsto \mathbb{R}^2$ denotes a dilatation map of weight λ defined by $(x,y) \mapsto (x,\lambda y)$, δ_n satisfies Eq. 29:

$$\tan(\delta_n) = -\frac{a_n}{b_n}\tan\left(\frac{\theta}{2}\right), \tag{29}$$

and k_n satisfies Eq. 30:

$$\sin^2((N+1)k_n) = \cos^2(\theta)\sin^2(k_n), \quad \text{for } 1 \le n \le 2N \tag{30}$$

In general, it is not possible to obtain explicit values for the distribution angles unless the case $\theta = 0$ or $\theta = \frac{\pi}{2}$ which are discussed in the next section. We can nevertheless give some hints on its structure. Indeed, for each twist angle θ, the Hückel distribution $\mathscr{D}_{Huckel}(N,\theta)$ of twisted $[N]$-cumulene by an angle θ possesses the following structure. The distribution $\mathscr{D}_{Huckel}(N,\theta)$ is such that (see Eq. 31):

$$\phi(N-z) - \phi\left(\frac{N}{2}\right) = \phi\left(\frac{N}{2}\right) - \phi(z), \;\; z = 0,\ldots,N \tag{31}$$

The distribution possesses an axis of symmetry directed along the vector $\phi(\frac{N}{2})$. As $\phi(0) = 0$ and $\phi(N) = \theta$, this axis is at $\frac{\theta}{2}$ or

10.1002/cphc.202200951
WILEY-VCH

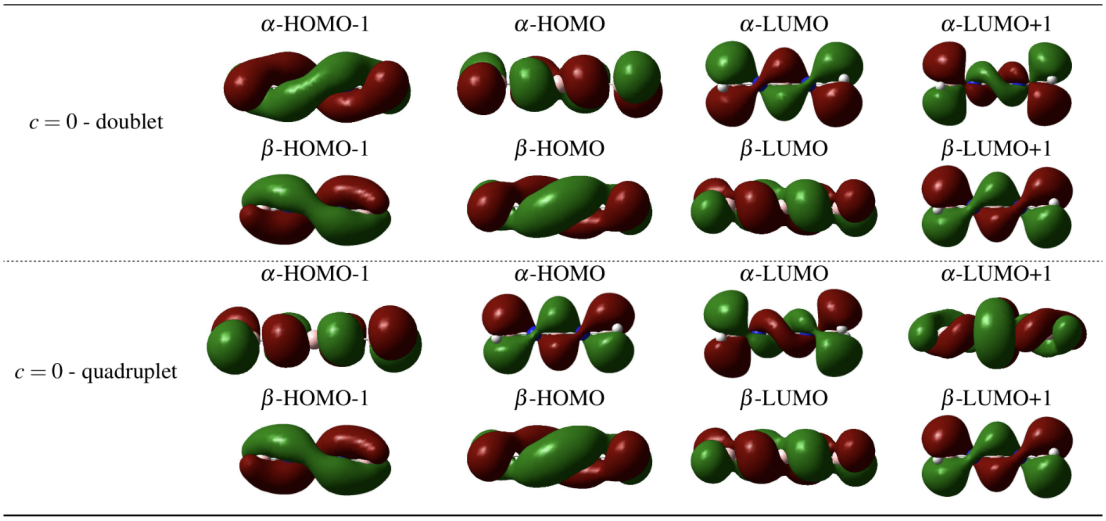

Figure 8. Molecular orbitals of a linear chain N=4 **B=N=B=N=B** obtained at the B3LYP/6-311G(d,p) level of theory - c = charge

$\frac{\theta}{2}+\frac{\pi}{2}$ depending on the number of turns and if the helix is right handed or left handed. It must be noticed that this property is not as trivial as it looks due to the fact that we have a dilatation map which sends the components of $\psi(z)$ on an ellipse as schemed in Figure 9.

The distribution is obtained from the circular distribution $\mathscr{D}_{circ}(\theta)$ defined by Eq. 32:

$$\phi_n(z) = k_n z + \delta_n \tag{32}$$

This distribution is symmetric with respect to 0, meaning that we have Eq. 33:

$$\phi_n(N-z) = -\phi_n(z), \tag{33}$$

for $z = 0,\ldots,N$. The distribution $\mathscr{D}_{Huckel}(\theta)$ is then obtained from $\mathscr{D}_{circ}(\theta)$ by a dilatation map $D_{b/a}$ from the vectors $v_n(z) = ae^{i\phi_n(z)}$, $i^2=-1$ followed by a rotation $e^{i\frac{\theta}{2}}$. Rotations are isometric transformations so that they preserve angles. Dilatations are not preserving angles, but they preserve the structure of the circular distribution as can be seen by a simple computation.

A **formal proof** of the previous result can be obtained **using the circularly polarized MOs** version of the previous case studied by S. Gunasekaran et al.[11] (p.4-5). They consider a modified Hückel matrix by increasing the coupling between the terminal lone p orbitals from t to $\sqrt{2}t$ instead of a constant coupling t between the atoms of the chain (see Fig. 5a p.5 in Ref. 11). This simple change made the mathematical analysis greatly simplified and explicit expressions for the distribution given by $\phi_n(0)=0$, $\phi_n(N)=\theta$ can be obtained (see Eqs. 34 and 35):

$$\phi_n(z) = k_n z, \quad z = 1,\ldots,N-1, \tag{34}$$

$$Nk_n = \begin{cases} \theta + m\pi, & n = 2m+1 \\ m\pi - \theta, & n = 2m \end{cases} \tag{35}$$

For a given $z \in \{1,\ldots,N-1\}$, we can rewrite $\phi_n(z)$ as Eq. 36:

$$\phi_n(z) = Nk_n\frac{z}{N} = \begin{cases} (\theta + m\pi)\frac{z}{N}, & n = 2m+1 \\ (m\pi - \theta)\frac{z}{N}, & n = 2m \end{cases} \tag{36}$$

The quantity $\phi_n(z)$ is well defined for $z=\frac{N}{2}$ and gives Eq. 37:

$$\phi_n(\frac{N}{2}) = \begin{cases} (\theta + m\pi)\frac{1}{2}, & n = 2m+1 \\ (m\pi - \theta)\frac{1}{2}, & n = 2m \end{cases} \tag{37}$$

We can verify directly the previous symmetry results on the distributions $\mathscr{D}_{Huckel}(\theta)$, *i.e.* that (Eq. 31) is satisfied. Indeed, we have Eq. 38:

$$\phi_n(\frac{N}{2}) - \phi_n(z) = \begin{cases} (\theta + m\pi)(\frac{1}{2} - \frac{z}{N}), & n = 2m+1 \\ (m\pi - \theta)(\frac{1}{2} - \frac{z}{N}), & n = 2m \end{cases} \tag{38}$$

and Eq. 39:

$$\begin{aligned} \phi_n(N-z) - \phi_n(\frac{N}{2}) &= \begin{cases} (\theta + m\pi)(1 - \frac{z}{N} - \frac{1}{2}), & n = 2m+1 \\ (m\pi - \theta)(1 - \frac{z}{N} - \frac{1}{2}), & n = 2m \end{cases} \\ &= \phi_n(\frac{N}{2}) - \phi_n(z) \end{aligned} \tag{39}$$

Properties of Distributions for C_2-Adapted MOs of $\theta = 0$ or $\theta = \frac{\pi}{2}$ Twisted Cumulene

For $\theta = 0$ or $\theta = \frac{\pi}{2}$, cumulenes do not possess helical MOs. This is due to the fact that the π_x-system and the π_y-system are decoupled in this case (see Basic Structural Properties for more details). However, we can look for C_2-adapted MOs, where C_2 mixes the π_x and π_y system.

Remark 5. *Looking for C_2-adapted MOs is natural when cumulenes are considered as linear versions of cyclic chains under the Möbius topology. This can be understood as* ***replacing the electronic complexity by a geometric complexity keeping symmetry properties*** *here given by a C_2 symmetry group. We refer to Ref. 1 for more details. In particular, one can note that the angular distribution for the Möbius cyclic system is perfect but this property is lost when looking for a cumulene analogue. We refer to Ref. 1 where this problem is studied in details and to the following sections.*

The Case $\theta = \frac{\pi}{2}$ For $\theta = \frac{\pi}{2}$, the π-system of cumulenes can be obtained by a N-chain of atoms from $z=0$ to $z=N-1$ governing the p_y part and a N-chain for p_x from $z=1$ to $z=N$. For a

10.1002/cphc.202200951
WILEY-VCH

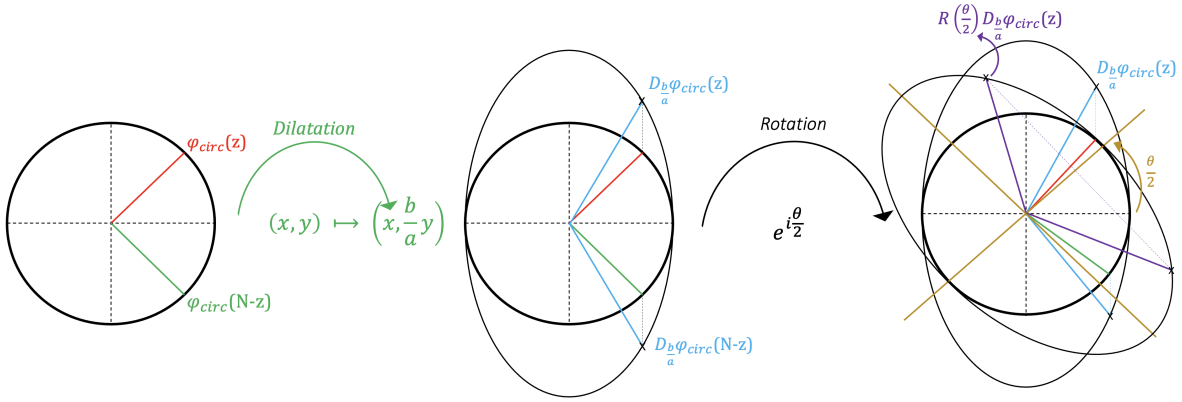

Figure 9. Construction of the helical distribution from the circular distribution

N-linear chain, the coefficients $c_{N,n}(z)$ of the wave function $\psi_n(z)$ for $z=1$ to N are of the form of Eq. 40:

$$c_{N,n}(z) = \sqrt{\frac{2}{N+1}}a_{N,n}(z) \tag{40}$$

where $a_{N,n}(z)$ is expressed as Eq. 41:

$$a_{N,n}(z) = \sin(k_n z), \quad z = 1,\ldots,N, \tag{41}$$

with k_n satisfying Eq. 42:

$$k_n = \frac{n\pi}{N+1}, \quad \text{for } 1 \le n \le N \tag{42}$$

The special form of the Hückel matrix in this case implies that (see The Case $\theta = \frac{\pi}{2}$ and Eqs. 43 and 44):

$$c_y(z) = \sqrt{\frac{2}{N+1}}a_{N,n}(z+1), \quad z = 0,\ldots,N-1, \tag{43}$$

$$c_x(z) = \sqrt{\frac{2}{N+1}}a_{N,n}(z), \quad z = 1,\ldots,N, \tag{44}$$

with $c_y(N) = 0$ and $c_x(0) = 0$. Looking for C_2-adapted MOs, we obtain Eqs. 45 and 46:

$$\psi_{+,n} = \frac{1}{\sqrt{2}}\left(c_y(z)p_y + c_x(z)p_x\right), \quad \text{and} \tag{45}$$

$$\psi_{-,n} = \frac{1}{\sqrt{2}}\left(c_y(z)p_y - c_x(z)p_x\right) \tag{46}$$

Choosing $\psi_{+,n}$ or $\psi_{-,n}$ give rise to a right (resp. left) hand helix. In the following, we focus on $\psi_{+,n}$. We then have Eq. 47:

$$\psi_n(z) = \sqrt{\frac{2}{N+1}}\begin{pmatrix} a_{N,n}(z) \\ a_{N,n}(z+1) \end{pmatrix} \tag{47}$$

For $z = 0,\ldots,N$, we want to compare $\phi_{+,n}(z)$ and $\phi_{+,n}(N-z)$. As the coefficients a_n satisfies Eq. 48:

$$a_{N,n}(N-z+1) = (-1)^{n+1}a_{N,n}(z), \tag{48}$$

(see A Technical Result) we deduce that $\psi_n(N-z)$ can be written as Eq. 49:

$$\begin{aligned}\psi_n(z) &= \sqrt{\frac{2}{N+1}}\begin{pmatrix} a_{N,n}(N-z) \\ a_{N,n}(N-z+1) \end{pmatrix} \\ &= (-1)^{n+1}\sqrt{\frac{2}{N+1}}\begin{pmatrix} a_{N,n}(z+1) \\ a_{N,n}(z) \end{pmatrix}\end{aligned} \tag{49}$$

As a consequence, $\psi_{+,n}(N-z)$ is obtained from $\psi_n(z)$ by axial symmetry along the line $y=x$ (diagonal symmetry) and multiplication by a factor $(-1)^{n+1}$. Denoting by $S:(x,y)\to(y,x)$ the diagonal symmetry map, we have Eq. 50:

$$\psi_{+,n}(N-z) = (-1)^{n+1}S(\psi_{+,n}(z)) \tag{50}$$

We directly deduce the relationship on the distribution of the angles Eq. 31. In this case (see The Case $\theta = \frac{\pi}{2}$), an explicit expression can be obtained for the angle $\mathscr{A}_{N,n,+,0,z}$ between $\psi_{+,n}(0)$ and $\psi_{+,n}(z)$ and is given by Eqs. 51 and 52:

$$\mathscr{A}_{N,n,+,0,z} = cos^{-1}\left(\varepsilon(a_{N,n}(1))\varepsilon(a_{N,n}(z+1))\frac{1}{\sqrt{1+\frac{a_{N,n}(z)}{a_{N,n}(z+1)}^2}}\right) \tag{51}$$

$$z = 0,\ldots,N-1, \tag{52}$$

and Eq. 53:

$$\mathscr{A}_{N,n,+,0,N} = (-1)^{n+1}\frac{\pi}{2}, \tag{53}$$

where $\varepsilon(x)$ denotes the sign of x. As an example, we obtain for $N=3$ and $N=4$ the distributions represented in Figures 10 and 11, respectively.

We can check some consequences of our previous results using the simulations, namely that:

- By Eq. 53, the angle between $\psi_n(0)$ and $\psi_n(N)$ is equal to $\frac{\pi}{2}$ when n is odd and $-\frac{\pi}{2}$ when n is even.
- For all n, the family of vectors $\psi_n(z)$, $z=1,\ldots,N$ are making a turn of an angle of $(2n-1)/4$ with respect to its initial position $\psi_n(0)$. As an example, for $N=3$, $n=1$ (a quarter turn), $n=2$ (three quarter turn) and $n=3$ (five quarter turn). In the same way, for $N=4$, $n=1$ (a quarter turn), $n=2$ (three quarter turn), $n=3$ (five quarter turn) and $n=4$ (seven quarter turn) etc.

The Case $\theta = 0$ For $\theta = 0$, the π-system of cumulenes can be obtained by a $N+1$-chain of atoms from $z=0$ to $z=N$ governing the p_y part and a $N-1$ chain for p_x for $z=1$ to $z=N-1$.

The special form of the Hückel matrix in this case implies that (see The Case $\theta = 0$ and Eqs. 54 to 57) :

$$c_y(z) = \sqrt{\frac{2}{N+2}}a_{N+1,n}(z+1) = \sqrt{\frac{2}{N+2}}\sin\left(\frac{n\pi(1+z)}{N+2}\right), \tag{54}$$

$$z = 0,\ldots,N \tag{55}$$

10.1002/cphc.202200951
WILEY-VCH

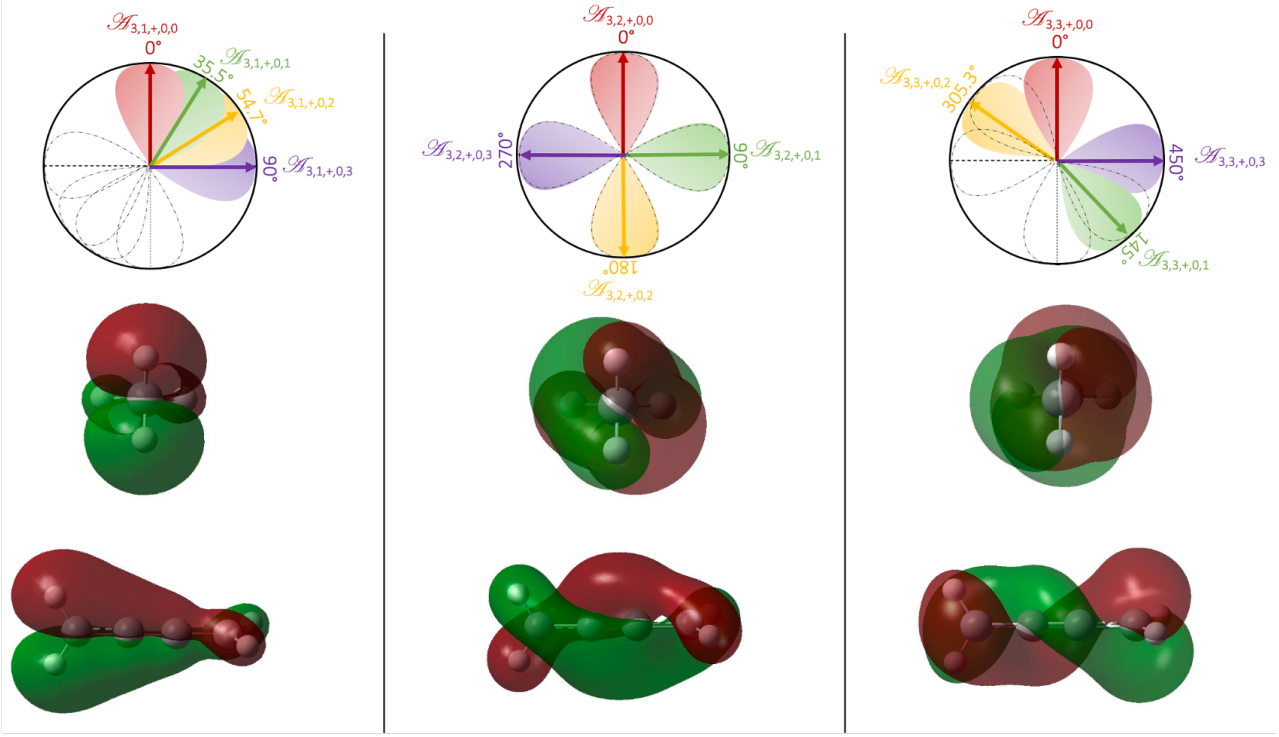

Figure 10. Distribution for $\theta = \frac{\pi}{2}$, $N = 3$, $n = 1$ (HOMO-2 and HOMO-3), $n = 2$ (HOMO-1 and HOMO) and $n = 3$ (LUMO and LUMO+1) - Corresponding MOs obtained by the CASSCF(8:10)/6-311G(d,p) level of theory for the [3]-cumulene in its excited triplet state (see Table S6 in Supporting Information for details).

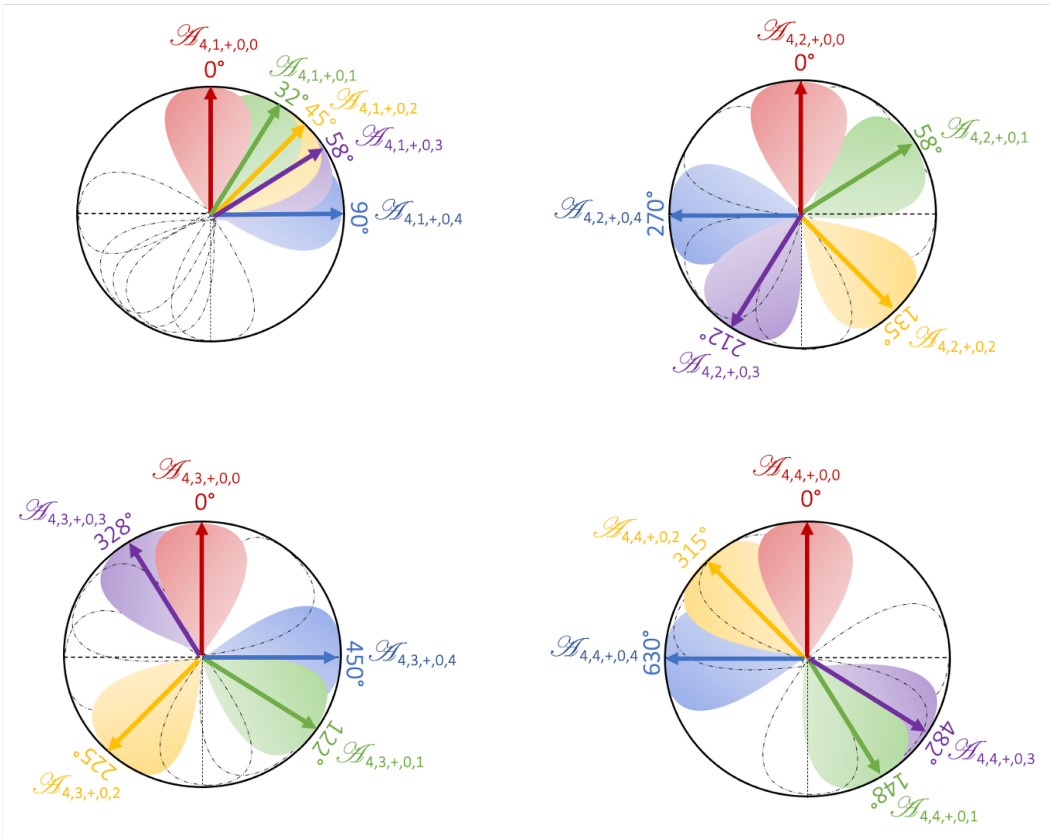

Figure 11. Distribution for $\theta = \frac{\pi}{2}$, $N = 4$, $n = 1$ (HOMO-2 and HOMO-3), $n = 2$ (HOMO-1 and HOMO), $n = 3$ (LUMO and LUMO+1) and $n = 4$ (LUMO+2 and LUMO+3)

10.1002/cphc.202200951
WILEY-VCH

$$c_x(z) = \sqrt{\frac{2}{N}} a_{N-1,n-1}(z) = \sqrt{\frac{2}{N}} \sin\left(\frac{(n-1)\pi z}{N}\right), \quad (56)$$

$$z = 1, \ldots, N-1, \quad (57)$$

with $c_x(0) = 0$ and $c_x(N) = 0$. Looking for C_2-adapted MOs, we obtain Eq. 58, focusing on $\psi_{+,n}$:

$$\psi_n(z) = \begin{pmatrix} \sqrt{\frac{2}{N}} \sin\left(\frac{(n-1)\pi z}{N}\right) \\ \\ \sqrt{\frac{2}{N+2}} \sin\left(\frac{n\pi(z+1)}{N+2}\right) \end{pmatrix} \quad (58)$$

for $z = 1, \ldots, N-1$. Here again, one can compute explicitly the distribution of angles for particular values of n. In particular, using the same notations as before, we have (see The Case $\theta = \frac{\pi}{2}$ and Eq. 59):

$$\mathscr{A}_{N,n,+,0,N} = \frac{(1-(-1)^{n+1})}{2}\pi = \begin{cases} 0 & \text{if } n \text{ is odd,} \\ \pi & \text{otherwise} \end{cases} \quad (59)$$

As an example, we obtain for $\theta = 0$, $N = 3$ and $N = 4$ the distributions depicted in Figures 12 and 13, respectively.

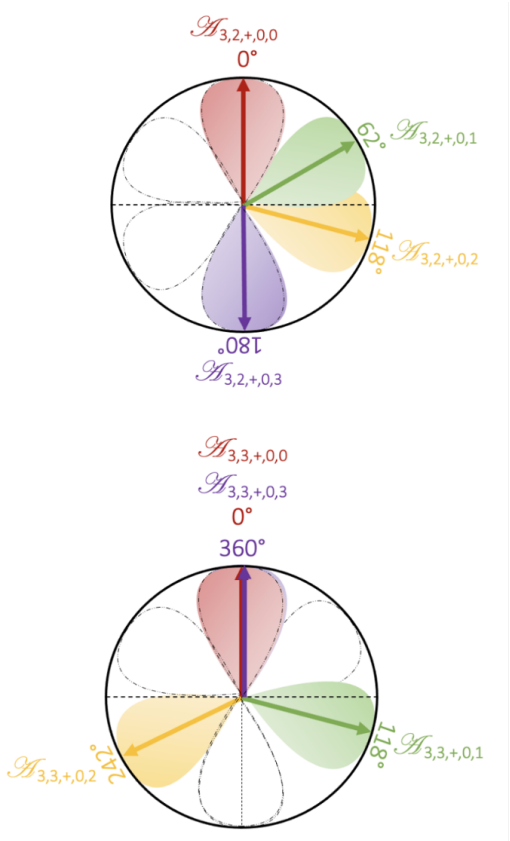

Figure 12. Distribution for $\theta = 0$, $N = 3$, $n = 2$ (HOMO-1 and HOMO), $n = 3$ (LUMO and LUMO+1)

The simulations illustrate our previous results:

- The angle between $\psi_n(0)$ and $\psi_n(N))$ is 0 when n is odd and 180 when n is even.
- For all n, the family of vectors $\psi_n(z)$ are making $(n-1)/2$ turns with respect to its initial position $\psi_n(0)$.In particular, for $N = 3$, $n = 2$ (half turn) and $n = 3$ (one turn). For $N = 4$, $n = 2$ (half turn) , $n = 3$ (one turn) and $n = 4$ (one and a half turns) etc.

Note that the results of distributions for $N = 11$ and $\theta = 10$ are illustrated in Figures S1-S3 in Supporting Information.

How To Detect Helical Orbitals - Algebraic Approach

Following S. Gunasekaran et al. in (Ref. 11, p.5-6), it is possible to detect helical orbitals in a pure **algebraic** way. The idea is to use the **Löwdin partitioning technique**[15], which is a simple technique allowing focus on a particular part of the molecule by "constructing an **effective Hamiltonian** which acts only on the target model space but gives the same result as the original Hamiltonian acting on the complete space" (see Ref. 16). The **Hamiltonian** H of the complete system can be written as Eq. 60:

$$H = \begin{pmatrix} H_{aa} & H_{aC} & 0 \\ H_{Ca} & H_{CC} & H_{Cb} \\ 0 & H_{bC} & H_{bb} \end{pmatrix} \quad (60)$$

The left group is associated to a set $p_a = (p_1, \ldots, p_a)$ of basis orbitals and the right group to $p_b = (p_1^\star, \ldots, p_b^\star)$. The central chain consists of $2N$ orbitals given by p_L, p_R and $2(N-2)$ orbitals $p_{x,i}$, $p_{y,i}$, $i = 1, \ldots, N-1$. We denote by p_C this vector. The matrix H is then a $a+2n+b$ square matrix. By construction of the Hamiltonian, we have $H_{Ca}^t = H_{aC}$ where t denotes the transpose. The associated **Schrödinger equation** $H \cdot \psi = E\psi$ gives for Eq. 61:

$$\psi = \sum_{i=1}^{a} c_i p_i + c_L p_L + \sum_{i=1}^{n} c_{x,i} p_{x,i} + c_{y,i} p_{y,i} + c_R p_R + \sum_{j=1}^{b} c_j p_j^\star \quad (61)$$

a linear system of the form of Eq. 62:

$$\begin{cases} H_{aa}p_a + H_{aC}p_C = Ep_a, \\ H_{Ca}p_a + H_{CC}p_C + H_{Cb}p_b = Ep_C, \\ H_{bC}p_C + H_{bb}p_b = Ep_b, \end{cases} \quad (62)$$

For any integer $d > 0$, let us denotes by I_d, the identity matrix of size d. Assuming that for a given E the matrices $EI_a - H_{aa}$ and $EI_b - H_{bb}$ are **invertible**, one can express p_a and p_b using p_C, as in Eq. 63:

$$\begin{cases} p_a = (EI_a - H_{aa})^{-1} H_{aC} p_C, \\ p_b = (EI_b - H_{bb})^{-1} H_{bC} p_C, \end{cases} \quad (63)$$

Replacing in the second equation p_a and p_b by their expressions, we obtain Eq. 64:

$$\begin{aligned} H_{Ca}(EI_a - H_{aa})^{-1} H_{aC} p_C \quad &+ \\ H_{CC} p_C \quad &+ \\ H_{Cb}(EI_b - H_{bb})^{-1} H_{bC} p_C \quad &= Ep_C \end{aligned} \quad (64)$$

This last equation can be understood as the action of an **effective Hamiltonian** H_{eff} defined over p_C by Eq. 65:

$$H_{eff} = \Sigma_L + H_C + \Sigma_R, \quad (65)$$

where the matrix Σ_L and Σ_R are defined by Eq. 66:

$$\begin{cases} \Sigma_L \quad = H_{Ca}(EI_a - H_{aa})^{-1} H_{aC} \\ \Sigma_R \quad = H_{Cb}(EI_b - H_{bb})^{-1} H_{bC}, \end{cases} \quad (66)$$

leading to a $2N \times 2N$ Hamiltonian. The two matrices $\Sigma_L(E)$ and $\Sigma_R(E)$ are $2N \times 2N$ and depend only on the coupling between the end groups and the terminal orbital of the chain p_L and p_R.

The main result of S. Gunasekaran et al.[11] can be stated as follows:

Existence criterion: *A necessary condition for H to yield helical states is that Σ_L and Σ_R do not commute, i.e. $[\Sigma_L, \Sigma_R] \neq 0$, where the bracket $[;]$ is defined by $[A,B] = AB - BA$.*

The main difficulty in applying this result is due to the computation of the two matrix Σ_L and Σ_R which leads **in general to**

10.1002/cphc.202200951
WILEY-VCH

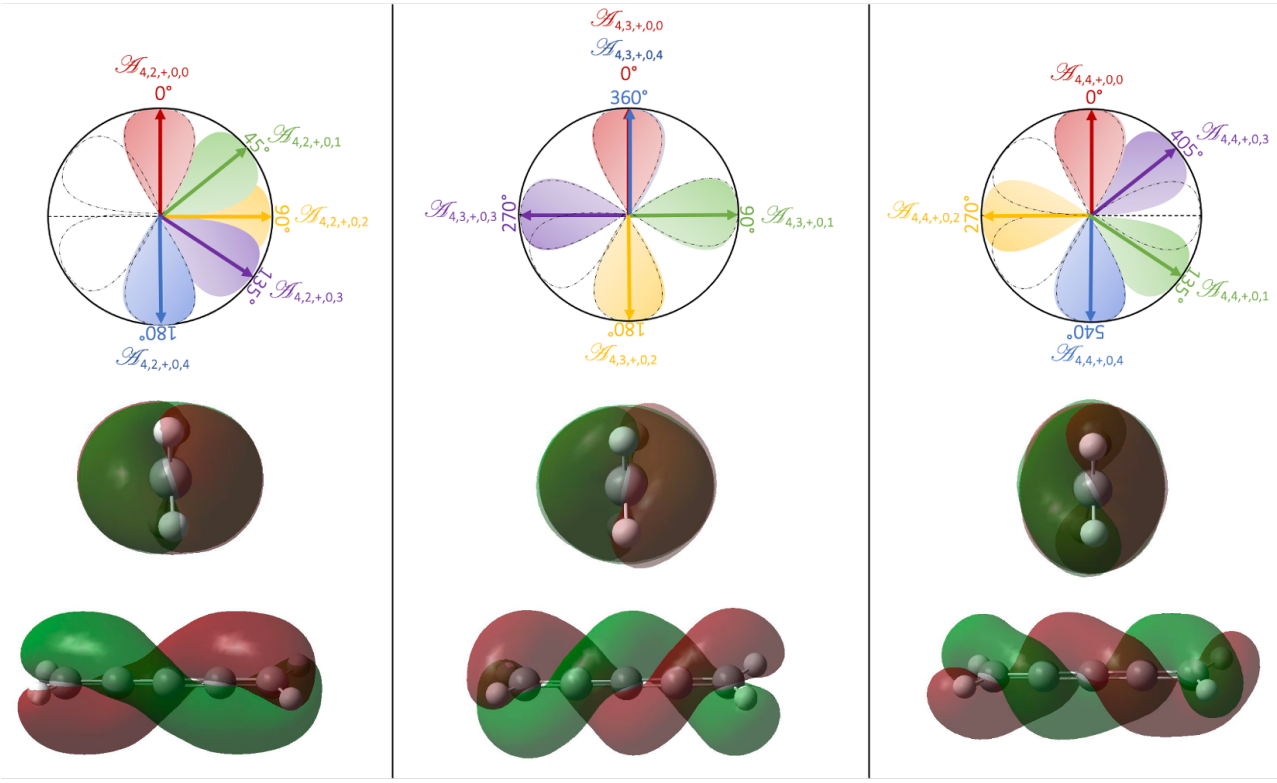

Figure 13. Distribution for $\theta = 0$, $N = 4$, $n = 2$ (HOMO-2 and HOMO-3), $n = 3$ (HOMO-1 and HOMO) and $n = 4$ (LUMO and LUMO+1) - Corresponding MOs obtained by B3LYP/6-311G(d,p) level of theory for the [4]-cumulene in its ground singlet state (see Table S7 in Supporting Information for details).

complex and non explicit expressions and only possible in simple configurations. We refer to Ref. 16 for more details and examples. However, we can deduce from the previous result the following statement:

Genericity of helical orbitals: *A linear chain satisfying the previous assumptions admits generically helical orbitals.*

The proof of this statement relies on the existence criterion. Indeed, let A and B be two arbitrary square matrices. The condition of non-commutation is open, *i.e.* that sufficiently small perturbations of A and B do not commute. Another way of saying that arbitrary close perturbations of commutative matrices are in general non-commutative. As a consequence, helical orbitals are not special; on the contrary they are the most common behavior of orbitals for linear chains.

Despite its interest, the previous criterion is from a practical point of view **not effective to detect helical orbitals** for a specific molecule as it demands the explicit computation of the matrices Σ_L and Σ_R. In the following, we rely on an approach suggested by Garner and co-workers in Ref. 1 making an essential use of the symmetry properties of the molecule.

How To Detect Helical Orbitals - Symmetries Approach

Basic Structural Properties

We restrict ourselves to linear molecules made of N atoms A_i, $i = 1,\ldots,N$. We denote by $\mathbb{A} = \{A_i\}_{i=1,\ldots,N}$ the family of atoms and by $L_{\mathbb{A}}$ the corresponding linear molecule. We assume that a coordinates system is given such that z is in the direction of the molecule. In order to observe helical MOs in a linear molecule $L_{\mathbb{A}}$, one needs to deal with atoms supporting a π-system which is two dimensional, *i.e.* with atoms having as a basis set p_x and p_y, p_z supporting the σ-bond. We assume that we have n such atoms. As a consequence, along the molecule we have two planes $\mathscr{P}_x$ and $\mathscr{P}_y$ containing the family of p orbitals $p_x(z)$ and $p_y(z)$ respectively where z denotes the integer position of each atom along the chain.

The previous restriction implies that one has to **restrict attention to atoms belonging to the bloc p of the periodic table of the elements**. Moreover, in order to have a structure which can be understood, it seems reasonable to restrict our attention to elements of the bloc p of the **second and third line of the periodic table**. The boundary of such a chain can be generated by a single MO. For more simplicity, we assume that the left boundary MO is $p_y = p_0$ and the right one is an MO denoted by p_N which can be arbitrarily oriented in the $x-y$ plane. We have then $N = n+2$ atoms in the linear chain. The left and right atoms of the linear chain belong to some structures denoted by S_L and S_R. The Hückel matrix of such a molecule takes the form in Eq. 67, taking as a basis set $p_0 = p_x$, p_x^i, p_y^i, $i = 1,\ldots,n$, p_N.

10.1002/cphc.202200951
WILEY-VCH

$$
\begin{array}{c}
\\ p_L \\ p_y^1 \\ p_y^2 \\ \\ \\ p_y^{N-1} \\ \\ p_r \\ p_x^{N-1} \\ \\ \\ \\ p_x^1
\end{array}
\begin{array}{c}
\begin{array}{ccccccccc} p_0^y & p_L & p_y & & p_y^{N-1} & p_R & p_x^{N-1} & & p_x^i \end{array} \\
\begin{pmatrix}
\alpha & a & 0 & \cdots & & & & & \\
a & & & & & & & & \\
0 & & A_y & & & 0 & & 0 & \\
\vdots & & & & & & & & \\
0 & & & & a & & & & \\
0 & & & a & \alpha & \odot^{\parallel} & 0 & 0 & \\
 & & 0 & & & & & & 0 \\
\vdots & & & 0 & \odot^{\parallel} & \alpha & \odot^{\perp} & 0 & \\
0 & 0 & \cdots & 0 & 0 & \odot^{\perp} & \alpha & a & \\
0 & & & & & & a & & \\
\vdots & & & & & & & & \\
\vdots & & 0 & & & 0 & & A_x & \\
0 & & & & & & & &
\end{pmatrix}
\end{array}
\tag{67}
$$

where the green, red and blue blocks denote the y-part, the mixing matrix and the x-part, respectively. The A matrix is given by Eq. 68:

$$
A_y = \begin{array}{c}
\\ p_y^1 \\ \vdots \\ p_y^k
\end{array}
\begin{array}{c}
\begin{array}{ccccc} p_y^1 & & \cdots & & p_y^k \end{array} \\
\begin{pmatrix}
\alpha & a & & & \\
 & \ddots & & 0 & \\
a & & & & \\
 & & \ddots & & a \\
 & 0 & & a & \alpha
\end{pmatrix}
\end{array}
\tag{68}
$$

The characteristic polynomial of H can be decoupled in two cases:

1. when $\odot^{\parallel} = 0$, corresponding to the case where p_N is orthogonal to p_x^n, *i.e.* $p_N = p_y$. The mixing matrix reduces to the orthogonal matrix shown in Eq. 69:

$$
Mix^{\perp} = \begin{pmatrix} \alpha & 0 & 0 \\ 0 & \alpha & \odot^{\perp} \\ 0 & \odot^{\perp} & \alpha \end{pmatrix} \tag{69}
$$

and the characteristic polynomial has the form of Eq. 70:

$$
P(x) = P_A(x) P_{A^{\perp}, \odot^{\perp}}(x). \tag{70}
$$

2. when $\odot^{\perp} = 0$, corresponding to the case where p_N is orthogonal to p_y^n, *i.e.* that $p_N = p_x$. The mixing matrix reduces to the one shown in Eq. 71:

$$
Mix^{\parallel} = \begin{pmatrix} \alpha & \odot^{\parallel} & 0 \\ \odot^{\parallel} & \alpha & 0 \\ 0 & 0 & \alpha \end{pmatrix} \tag{71}
$$

and the characteristic polynomial is given by Eq. 72:

$$
P(x) = P_{A^{\perp}}(x) P_{A, \odot^{\parallel}}(x). \tag{72}
$$

The first case corresponds to the orthogonal configuration of the ethylene and the second one to the planar configuration. In all the other configurations, we have a mixing between the components of the p_x and p_y orbitals which is a necessary condition for the existence of helical orbitals.

Symmetry Properties

The existence of helical states implies that we have a mixing between MOs p_x and p_y in a very special way. In particular, we assume that there exists what is called an **helicogenic C_2 symmetry axis** (see Ref. 1), *i.e.* a C_2 axis such that $C_2(p_x) = p_y$.

As an example, for the ethylene we have:

- the planar configuration of the ethylene possesses three C_2 axes: one directed along the chain and two passing through the centre directed along x and y. None of these C_2 axes are helicogenic.
- the orthogonal configuration also possesses three C_2 axes: one along the chain and two which are dihedral. These last two axes are helicogenic.

However, as already discussed in the previous section, none of these two examples possess explicit helical MOs. In the first case, no mixing is induced by the symmetries so that one cannot wait for helical MOs. For the orthogonal case however, this is due to the fact that despite the mixing generated by the symmetry axes, the characteristic polynomial factorizes and the behaviour of the p_x and p_y family is disconnected. This last property can be related to the existence of another symmetry of the molecule, namely that the orthogonal configuration of the ethylene possesses a **mirror-plane symmetry**. As a consequence, we have to assume that no mirror-plane symmetry must be present in order to generate helical MOs.

The Helical Orbitals Criterion - Symmetries

Following the previous discussion, we are led to the following statement, which was originally made by M. H. Garner et al.[1] (p. J) for cumulenes:

The helical orbitals criterion: *Linear chain $L_{\mathbb{A}}$ satisfying the structural assumption, without mirror-plane symmetry, admitting a C_2 helicogenic axis, has explicit helical MOs.*

The proof of such a theorem can be deduced from the properties of the Hückel matrix associated to such kind of molecules. The absences of a mirror-plane symmetry implies that the molecule is **chiral**, *i.e.* that the image of the molecule by a mirror plane is not invariant. This remark can be used to give an alternative statement of the helical orbitals theorem:

Helical orbitals criterion: *linear chain $L_{\mathbb{A}}$ satisfying the structural assumption and chiral admitting a C_2 helicogenic axis, has explicit helical MOs.*

This statement can be related to the **Curie's principle** in which he states informally in his paper "On Symmetry in Physical Phenomena"[17] in 1894 an intuitively plausible relationship between the symmetry of an effect and its cause, namely that "when certain causes produce certain effects, the elements of symmetry of the causes must be found in the effects produced" (p. 401). Indeed, we are waiting for helical molecular orbitals. These objects are naturally chiral so that following Curie's principle, one must find chirality in the initial geometry of the molecule which induces the orbitals structure. As a consequence, chirality is unavoidable. The Curie's principle gives a physical support to the sentence "the formation of helical symmetry-adapted MOs requires chirality; not surprising considering a helix is a chiral object" made by M.H. Garner et al. in ([1], page J): this is not surprising indeed and is a consequence of the Curie's principle. We refer to Chalmers' as well as Ismael's investigations[18,19] for more details and discussion about the validity of the Curies's principle.

Observable Consequence of the Helicity

One of the electronic property strongly depending on the absolute structure of the $[N]$-cumulene and their dihedral angles θ-value between the two CH_2 end groups is the optical rotation β-response

property. Another relationship observed between helicity and observable (magnetism) will be discussed in Beyond ***p***-Orbitals - Helical States Using ***d***-Orbitals and Metallacumulenes.

In solution or gaz phase, the molecule is optically active if the trace of its optical rotation is not equal to zero, *i.e.* for the C_2 symmetry and when θ is neither equal to 0 (D_{2h} symmetry) nor 90°(D_{2d} symmetry) *i.e.* the conditions required to turn off the helical orbital criterion as established in Symmetry Properties.

In Table 1, we have reported the $\bar{\beta}$ mean optical rotation value of methane, ethylene and $[N]$-cumulene (in its singlet state) with $[N]$ equal to 2, 3,... and 5, and for θ equal to 0, 10, 20, ... and 90°, at the light wavelength equal to 1000 nm (1.24 eV) making negligible its vibrational contribution.

First, the self-consistent field (SCF) PBE0 hamiltonian with the 6-31G** basis set is used to calculate the unperturbed singlet state. Then, the frequency-dependent coupled-perturbed (CP-PBE0) method is used with the velocity operator as the electric field perturbation. In that condition, it is shown that the trace is gauge-invariant[20].

It is interesting to see that $\bar{\beta}$ is larger for small values of θ (except 0°per symmetry reason) for even $[N]$-number, and decreases to zero when the angle increases till 90°. This is due to the fact that the HOMO $\rightarrow$ LUMO ΔE-energy (not reported in the table) increases when θ increases. This is exactly the contrary for odd $[n]$-number: ΔE decreases when θ increases, and $\bar{\beta}$ is larger for large values of θ (except 90°per symmetry reason). However, for [3] and [5], the CP-PBE0 optical gap is reached with 1.24 eV ($\lambda = 1000$ nm) when θ is between 70 and 80°, and 60 and 70°, respectively. Actually, the unrelaxed HOMO $\rightarrow$ LUMO ΔE energy is around 2 eV for these previous structures, but the CP-PBE0 calculation diminishes the optical gap by an exciton energy correction of ~ 1 eV with respect to the unrelaxed sum over state PBE0 (SOS-PBE0) one. This is the reason why $\bar{\beta}$ becomes very large (in absolute values) and changes its sign after resonances. It is important to notice that for θ larger than 90°, the sign of $\bar{\beta}$ changes since the other enantiomer forme is obtained.

Induced Helical MOs for Non Helical Linear Chains

The previous characterization of helical MOs can be used to induce helical states from a molecule which does not admit it at a first glance. Several strategies can be tested.

Breaking of Symmetries and Chirality

Let us consider a linear chain which does not satisfy the helical orbital criterion but satisfying the structural assumptions. By definition, the core chain possesses two C_2 helicogenic axes and one C_2 axis along the chain. Moreover, the core chain also possesses also three orthogonal mirror planes $\sigma_{x,y}$, $\sigma_{x,z}$ and $\sigma_{y,z}$ (see Figures 14 and 15 - the choice of x and y axes defined in these two figures is the one chosen for all the MOs representations of this article).

In order to satisfy the helical orbital criterion, we have to break the mirror-plane symmetries. This will depend on the fragment we put on the boundaries. This can be done in several steps:

- Breaking the $\sigma_{x,z}$ mirror-plane symmetry means that the molecule is not planar.

Let us now consider a non-planar linear chain. This condition is not sufficient as the orthogonal configuration of the $[N]$-cumulenes in their ground states does not support helical MOs for example.

- Taking the left fragment L to be contained in the plane $\sigma_{x,z}$, the breaking of the mirror-plane $\sigma_{x,z}$ will be effective with a **right fragment R which is not contained in $\mathscr{P}_y$**.

Such a choice, will naturally induce the breaking of the $\sigma_{x,y}$ mirror-plane symmetry. The previous remarks imply that an **axis torsion** of the end group of a linear chain will **generically induce helical MOs**.

Using Exited States of Molecules

The previous result is valid as long as one considers a stable minimal configuration, *i.e.* the fundamental configuration of a given molecule. However, the **symmetry group of the MOs of a given molecule depends on its energy state**. As a consequence, if the symmetry group of a given molecule is such that the molecule does not admit helical MOs but contains symmetry elements which alone satisfy the helical state theorem, one can find an **excited versions** of it, which can nevertheless **exhibit helical MOs** thanks to **symmetry adapted MOs** (see Figures 16 and 17). As we see, the previous remark also applies also for **different electronic multiplicities**. In the next section, we study more complex examples illustrating the previous discussion. In particular, we observe the following results:

- There exists generically excited version of the molecule leading to stable configuration admitting helical states.
- Symmetry adapted MOs can be used to predict the characteristics of the helixes.

Cumulenes Containing Double-Bonded Heavy Elements

Cumulenes are a highly varied class of compounds, including such species as ketenes, allenes, ketenimines, and isocyanates, as well as analogues where carbons C_0 and C_N are replaced by silicon, germanium, oxygen, sulfur, nitrogen phosphorus and/or arsenic (see Figures 18 and 19).

In agreement with the review of Escudié et al.[21] fifteen families of compounds were studied in order to scan a major part of the experimentally known cumulenes containing double-bonded heavy elements. Examples of molecules (see Table 2) were tested at the B3LYP/6-311G(d,p) level of theory in order to study the presence of helical orbitals. Note that 2 other examples with DPBD and tolanophane molecules demonstrate also induced helical MOs are visible in Figures S9 and S10 in Supporting Information.

Beyond ***p***-Orbitals - Helical States Using ***d***-Orbitals and Metallacumulenes

As recently reported by Garner et al.[10] the prospective of helical states using d-orbitals has started. In particular, the metallacumulenes are potential classes of molecules that may exhibit helical MOs in the linear fragments of the molecules. If some MOs of the trans-$[EtC=(C=)_4C=Ru=(C=)_4CMe]^{2+}$ system are somewhat helical, Garner also reports that at the ruthenium centre there exists a jump not yet identified in the evolution of the helical MOs. This jump is assigned by the authors to the inherent sign-change in the metal d-orbitals that couple to the carbon π-orbitals.

The presence of variable helicity in different parts of a molecule is then clearly highlighted. However, the question that now arises is whether the existence of possible helical MOs of the metal part. In a last perspective we finally wanted to imagine the helical MOs of the metallic part through, for example, the study of a metal-metal bonds. Theoretical investigations refer to the existence of

10.1002/cphc.202200951
WILEY-VCH

Table 1. CP-PBE0 optical rotation ($\bar{\beta}$) of methane, ethylene and [N]-cumulene (singlet state) in degree dm^{-1} mol.$^{-1}$ l. with respect to the dihedral θ-angle in degree. The light wave length is: $\lambda = 1000$ nm (1.24 eV).

θ	0	10	20	30	40	50	60	70	80	90
methane / $\bar{\beta}$	0.0	1.2	2.0	1.9	1.4	0.9	0.4	0.1	0.0	0.0
ethylene / $\bar{\beta}$	0.0	4.0	9.0	15.0	21.0	30.0	40.0	50.0	13.0	0.0
[2]-cumulene / $\bar{\beta}$	0.0	15.0	13.0	11.0	10.0	8.0	6.0	4.0	2.0	0.0
[3]-cumulene / $\bar{\beta}$	0.0	7.0	15.0	25.0	39.0	60.0	100.0	248.0	−123.0	0.0
[4]-cumulene / $\bar{\beta}$	0.0	22.0	17.0	14.0	11.0	8.0	6.0	4.0	3.0	0.0
[5]-cumulene / $\bar{\beta}$	0.0	19.0	40.0	71.0	122.0	216.0	313.0	−71.0	−306.0	0.0

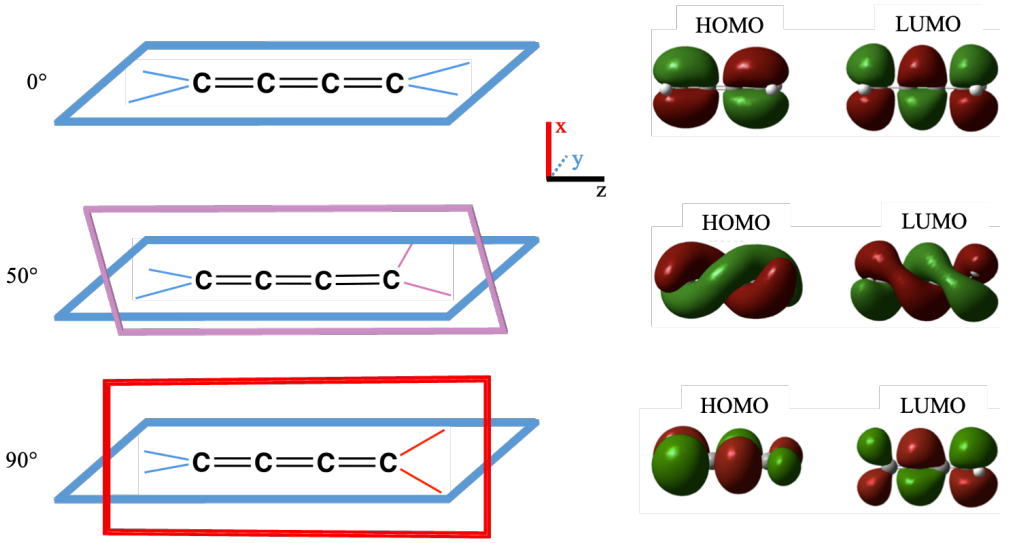

Figure 14. Representation of the HOMO and LUMO MOs obtained at the B3LYP/6-311G(d,p) level of theory for the $N = 3$ cumulene in its ground singlet state at a 0°, 50°and 90°rotation (see Table S5 in Supporting Information for details).

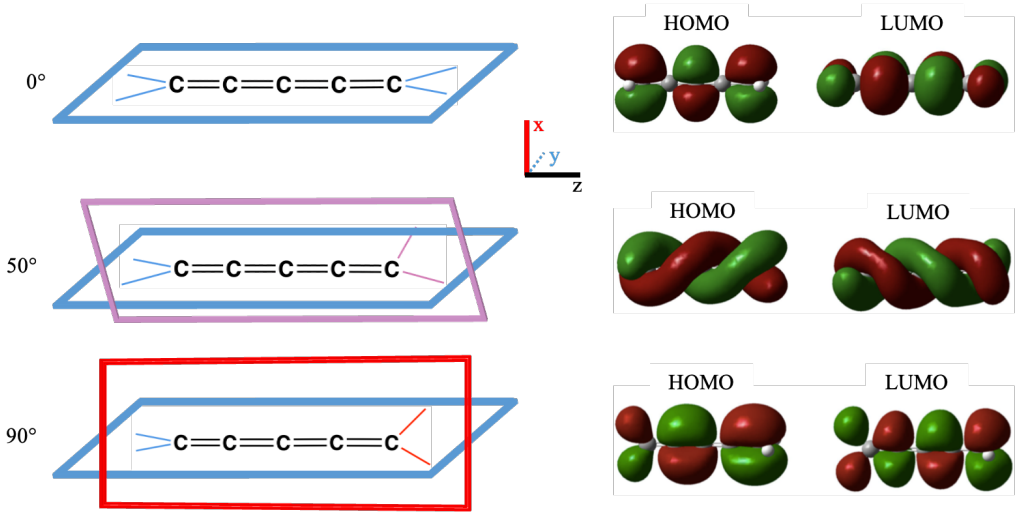

Figure 15. Representation of the HOMO and LUMO MOs obtained at the B3LYP/6-311G(d,p) level of theory for the $N = 4$ cumulene in its ground singlet state at a 0°, 50°and 90°rotation (see Table S7 in Supporting Information for details).

multiple metal-metal bonds, mainly consisting of a combination of σ and π interactions in all the $[M_2X_8]^{2-}$ species investigated[22]. In addition, δ-like interactions also occur in the complexes of rhenium (M=Re) in particular. The conformation of the $[Re_2H_8]^{2-}$ system where hydrogen ligands are eclipsed (D_{4h}) were studied in its lowest energy configuration represented as $[\sigma^2\pi^4\delta^2]$. The main reason of this decision was that conformation allows for maximum δ-δ overlap between the Re(III) centre resulting in the formation of a potential helix when the (D_{4h}) symmetry is broken as shown in Figure 20.

10.1002/cphc.202200951
WILEY-VCH

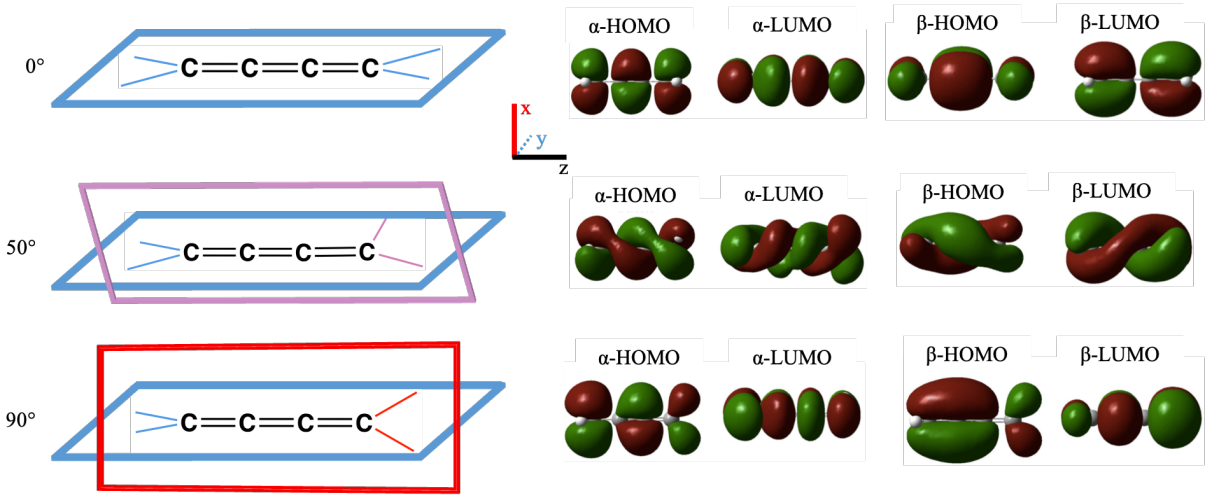

Figure 16. Representation of the HOMO and LUMO MOs obtained at the B3LYP/6-311G(d,p) level of theory for the $N = 3$ cumulene in its first excited triplet state at a 0°, 50°and 90 °rotation (see Table S6 in Supporting Information for details).

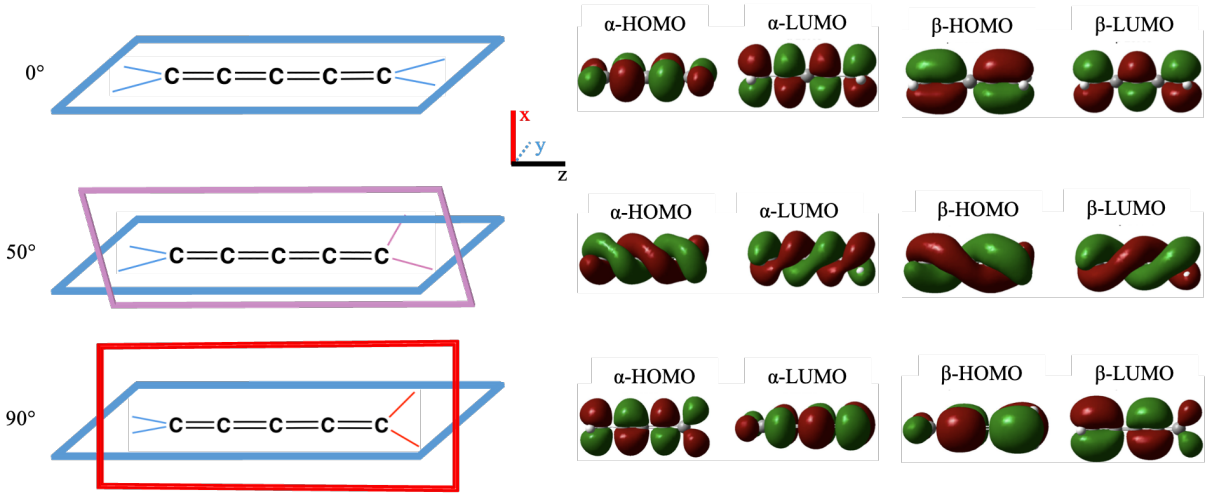

Figure 17. Representation of the HOMO and LUMO MOs obtained at the B3LYP/6-311G(d,p) level of theory for the $N = 4$ cumulene in its first excited triplet state at a 0°, 50°and 90°rotation (see Table S8 in Supporting Information for details).

Following a recent result presented by Gendron et al.[23] we discuss another possibility of using metallacumulenes. The main observation is that thanks to δ interaction and breaking of symmetries, helical orbitals are again observed. Interestingly, another possible arrangement of metallacumulenes consists in positioning two metallic fragments as end-groups. These systems have been developed originally as models of molecular wires following the early developments of molecular electronics[24]. The electron-rich metallic fragments that are usually found in the literature are of general formula ML_n (M = Fe, Ru, Re essentially; L = organic or inorganic coordinating ligands). They are connected to the carbon atoms via a direct metal-carbon bond. Depending on the oxidation state of the systems, the carbon chains that are encountered can be described as polyynediyl (L_nM-$(C_2)_x$-ML_n) type with a different amount of cumulene character. Interestingly, the electronic structures of this compounds can comprise helical carbon-chain MOs depending on the local symmetry of the ML_n fragments (usually pseudo-octahedral), their orientations, and the degree of cumulene-type character[23,25,26]. In the $[Cp^*(dppe)M\text{-}(C_2)_3\text{-}M(dppe)Cp^*]^{m+}$ series (Cp^* = pentamethylcyclopentadienyl; dppe = (diphenylphosphinno)ethane); M = Fe, Ru; $m = 0, 1, 2$), the two-electron oxidized unsaturated systems (m = 2) are presenting interesting magnetic behaviors in which the symmetry-breaking induced by the rotation of one metallic end-groups with respect to the other has a direct consequence on the magnetic coupling, *i.e.* on the relative energies between the ferromagnetic and the antiferromagnetic states[23,25]. Interestingly, the spinorbitals which are mainly involved in the description of the unpaired electrons are showing a twisted shape which seems to reinforce the antiferromagnetic coupling[5,6]. This will be investigated following this fundamental study (see preliminary results in Supporting Information).

Conclusion

Starting from the work of M. H. Garner et al.[1], we studied in generality the generation of helical orbitals for particular chain of atoms which include in particular $[N]$-cumulenes.

We first discuss the definition of helical orbitals following Ref. 1,11. In particular, we discuss the possibility to associate a perfect helix to a given distribution of angles representing the evolution of the π-system along the chain. We introduce as an index of helicity

10.1002/cphc.202200951
WILEY-VCH

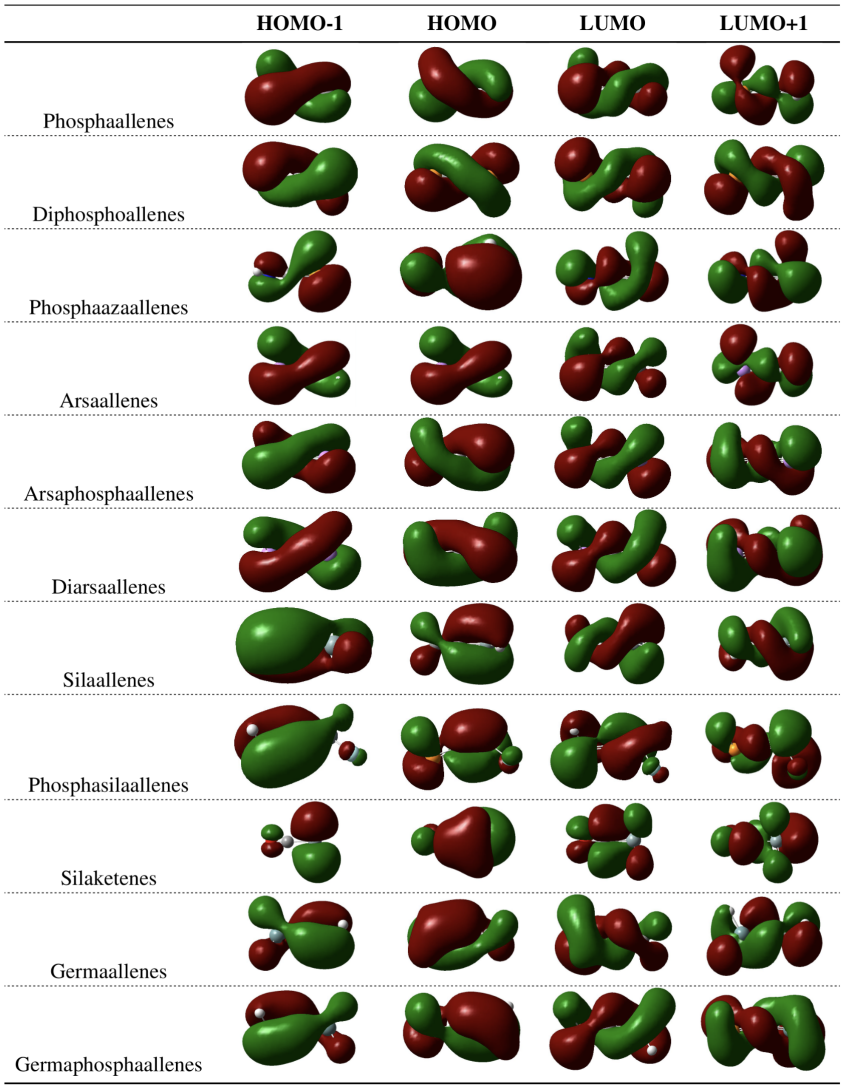

Figure 18. $N = 2$. Molecular orbitals obtained at the B3LYP/6-311G(d,p) level of theory for a rotation of 25°.

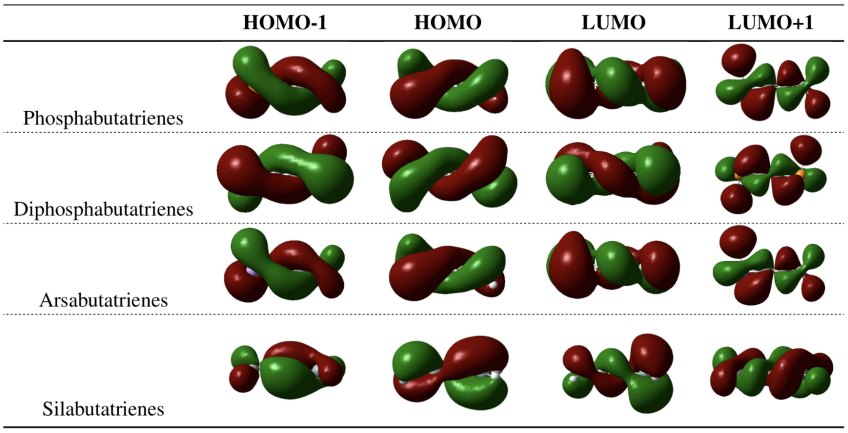

Figure 19. $N = 3$. Molecular orbitals obtained at the B3LYP/6-311G(d,p) level of theory for a rotation of 25°.

a correlation number obtained by linear regression between an hypothetical perfect helix and the exact feature of the π-system under consideration. This index is different from the MAD index of Ref. 10. Taking as an example linear chains of boron nitride, we show that perfect helix are not the rule and a more general definition of helices are needed, as long as one is interested in characterizing as precisely as possible helical orbitals by a single parameterized function.

10.1002/cphc.202200951
WILEY-VCH

Table 2. Cumulenes containing doubly bonded heavy elements - see figure **1** for the L_1, L_2, R_1 and R_2 definitions.

	A_0/A_N	L_1	L_2	R_1	R_2
Cumulene	C/C	H	H	H	H
N=3 :					
Phosphabutatriene	P/C	H	-	H	H
Diphosphabutatriene	P/P	H	-	H	-
Arsabutatriene	As/C	H	-	H	H
Silabutatriene	Si/C	H	H	H	H
N=2 :					
Phosphaallene	P/C	H	-	H	H
Diphosphaallene	P/P	H	-	H	-
Phosphaazaallene	P/N	H	-	H	-
Arasaallene	As/C	H	-	H	H
Arsaphosphaallene	As/P	H	-	H	-
Diarsaallene	As/As	H	-	H	-
Silaallene	Si/C	H	H	H	H
Phosphasilaallene	Si/P	H	H	H	-
Silaketene	Si/O	H	H	-	-
Germaallene	Ge/C	H	H	H	H
Germaphosphaallene	Ge/P	H	H	H	-

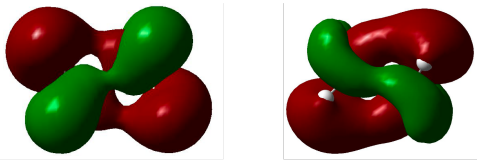

Figure 20. Representation of the N=1 HOMO-5 and the HOMO of the $[Re_2H_8]^{2-}$

We then give a global description of distribution obtained using Hückel theory for twisted $[N]$-cumulenes generalizing and completing previous work of M. H. Garner et al.[1] which is limited to even numbered $[N]$-cumulenes. Explicit formula are given and several general properties of Hückel-distribution are proved. Simulations are provided in order to illustrate these properties.

We then discuss minimal assumptions under which a given linear chain admit helical orbitals. Several methods exist.

We first focus on an algebraic characterization of helical orbitals given by S. Gunasekaran et al.[11] based on the Löwdin partitioning technique. Using this characterization, we deduce that helical orbitals are generic. Indeed, the existence criterion is based on the fact that two matrices do not commute which is a generic property for a set of matrices. Despite its interest, this criterion is not useful from a practical point of view because the computation of the matrices entering in the criterion are in general too complicated to compute explicitly.

We then discuss more precisely the structural properties of linear chain focusing on the role of symmetries of the molecule. As helical orbitals are associated to special geometrical properties of the molecule and are chiral objects, we deduce using Curie's principle, that a necessary condition for a molecule to possess helical orbitals is chirality. This assumption joins observation made by M. H. Garner et al.[1]. Moreover, the existence of helicogenic axes of symmetries as defined in Ref. 1 is also necessary. The previous conditions are necessary when looking for helical orbitals at the ground state. If not, as the symmetry group of MOs for a given molecule depends on the energy state, one can look for excited version of a given molecule for which symmetry adapted MOs lead to helical orbitals. The previous remark opens many possibilities for a huge number of structures to exhibit helical orbitals, in particular when different electronic multiplicities are allowed. This point clearly proves again that helical orbitals must be more generic than usually believed. Several examples are given in order to illustrate these ideas.

Helical orbitals are constructed by focusing on $2p$ orbitals. However, the criterion for helicity based on helicogenic axes and chirality suggests that d orbitals can be a good candidate to construct helical orbitals of a new kind. Following a recent result presented in Ref. 10 we discuss this possibility using metallacumulenes. The main observation is that thanks to δ interaction and breaking of symmetries, helical orbitals are again observed.

We hope that this work provides significant information and tools to study helical orbitals in various situations. The use of d-orbitals seems to be very promising as it opens the possibility to construct helical orbitals for new types of molecules with possibly different helical morphology.

Computational Methods

In the same way that Garner et al. asked the following question e.g. "What changes if we progress from a Hückel model to wave function based or DFT calculations?"[1], it is legitimate to ask the same type of question concerning eventual changes observed by the use of approaches leading to the use of the multiconfigurational wave function on the one hand and, by the use of purely localized orbitals and/or unlocalized model in other hand. To do this, it is important to situate the methods in relation to each other.

In this work, the ground and excited-states geometries were all determined at the DFT level using the B3LYP exchange-correlation function with the 6-311G(d,p) basis set. Calculations were performed using Gaussian 09 program package[27]. To describe an

10.1002/cphc.202200951
WILEY-VCH

eventual Multi-Reference character of states, CASSCF(8:10)sp/6-311G(d,p) calculations were also carried out. CASSCF calculations were performed using Molpro program package[28].

As expected, mono and pluri-determinental wavefunctions reach to the same conclusions. It is the same for calculations with different orbital representations e.g., delocalized and localized (see Tables S1 and S2 in Supporting Information). Two series of calculations have been carried out to highlight this assumption. Plane-wave delocalized orbitals calculations were performed using DFT within the augmented wave projector approach, as implemented in the VASP software[29–31].The basis set expansion is fixed by a cut-off energy of 550 eV, and the PBE exchange-correlation functional was used. Simulations were carried out on isolated molecules into a ∼8000 Å^3 box to remove any interaction between periodic images. Only the Γ-point was considered to describe the first Brillouin zone. Results on $N=3$ and $N=4$ of the cumulene systems were carried out and are reported in Supporting Information(see Tables S5-S8). There is no noticeable change between the MOs obtained by this approach and those obtained classically in B3LYP/6-311G(d,p).

Second, because the occupied canonical orbitals that are obtained from a Hartree-Fock (HF) calculation are generally delocalized, it could be difficult to attach a chemical interpretation to these molecular orbitals. The set of canonical molecular orbitals can be transformed into equally valid set of localized HF molecular orbitals by a (unitary) transformation that preserves orthonormality. These localized molecular orbitals (LMOs)[32] correspond to chemically familiar concepts, including the core orbitals on the heavy atoms, bonding orbitals, and the lone pair orbitals. As illustrate in Supporting Information (Tables S1 and S2) each localized orbital obtained for the cumulene systems will have a partial twist to recover the overall twist of the wavefunction. For localized natural orbitals (LNO), the obtained solutions must be mixed (±) into a linear combination (50/50) to reconstruct the twist (right/left) of the wavefunction to recover the helical character (see Figure 21).

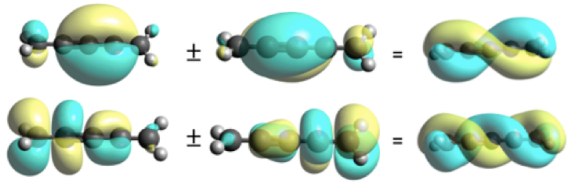

Figure 21. Combination of molecular HOMO-1 ± HOMO and LUMO ± LUMO+1 orbitals of cumulene with $N=4$ with localized natural orbitals in B3LYP/6-311G(d,p), + clockwise, - unclockwise

Appendix

A Technical Result

For all $N \geq 1$, $z=0,\ldots,N$, the function $a_n(z)=\sin\left(\frac{zn\pi}{N+1}\right)$ satisfies the equality in Eq. 73:

$$a_n(N-z+1)=(-1)^{n+1}a_n(z) \tag{73}$$

This is a simple computation. We have Eq. 74:

$$\begin{aligned} a_n(N-z+1) &= \sin\left((N-z+1)\frac{n\pi}{N+1}\right) \\ &= \sin\left(\frac{(N+1)n\pi}{N+1}-\frac{zn\pi}{N+1}\right) \\ &= \sin(n\pi)\cos\left(\frac{zn\pi}{N+1}\right)-\cos(n\pi)\sin\left(\frac{zn\pi}{N+1}\right) \\ &= -\cos(n\pi)\sin\left(\frac{zn\pi}{N+1}\right)=(-1)^{n+1}a_n(z) \end{aligned} \tag{74}$$

Proof of the Angle Formula for Cumulene

The Case $\theta=\frac{\pi}{2}$

The aim of this section is to prove the following formula in Eq. 75:

$$\begin{aligned} \mathscr{A}_{N,n,+,0,z} &= \cos^{-1}\left(\frac{\psi_n(0).\psi_n(z)}{\|\psi_n(0)\|\|\psi_n(z)\|}\right) \\ &= \cos^{-1}\left(\frac{\varepsilon(a_n(1))\varepsilon(a_n(z+1))}{\sqrt{1+(a_n(z)/a_n(z+1))^2}}\right) \end{aligned} \tag{75}$$

where $\varepsilon(x)$ is the function equal to $+1$ if $x>0$ and -1 if $x<0$.

The two vectors $\psi_n(0)$ and $\psi_n(z)$ are given by Eq. 76:

$$\begin{cases} \psi_0(z) = \sqrt{\frac{2}{N+1}}\begin{pmatrix} 0 \\ a_n(1) \end{pmatrix} \\ \psi_n(z) = \sqrt{\frac{2}{N+1}}\begin{pmatrix} a_n(z) \\ a_n(z+1) \end{pmatrix} \end{cases} \tag{76}$$

whose scalar product $\psi_n(0)\cdot\psi_n(z)$ is given by Eq. 77:

$$\psi_n(0)\cdot\psi_n(z)=\frac{2}{N+1}a_n(1)a_n(z+1) \tag{77}$$

The norm of each vector $\psi_n(0)$ and $\psi_n(z)$ is given by Eqs. 78 and 79:

$$\|\psi_n(0)\|=\sqrt{\frac{2}{N+1}}\,|\,a_n(1)\,| \quad \text{and} \tag{78}$$

$$\|\psi_n(z)\|=\sqrt{\frac{2}{N+1}}\sqrt{(a_n(z))^2+(a_n(z+1))^2} \tag{79}$$

We then obtain Eq. 80:

$$\mathscr{A}_{N,n,+,0,z}=\cos^{-1}\left(\frac{a_n(1)a_n(z+1)}{|\,a_n(1)\,|\,\sqrt{(a_n(z))^2+(a_n(z+1)^2}}\right) \tag{80}$$

As $a_n(z+1)\neq 0$ when $z=1,\ldots,N-1$, putting $(a_n(z+1))^2$ in factor in the square root, we deduce Eq. 81:

$$\mathscr{A}_{N,n,+,0,z}=\cos^{-1}\left(\varepsilon(a_n(1))\varepsilon(a_n(z+1))\frac{1}{\sqrt{1+\frac{(a_n(z)}{a_n(z+1))}^2}}\right) \tag{81}$$

When $z=N$, we have $a_n(N+1)=\sin(n\pi)=0$ and $\mathscr{A}_{N,n,+,0,N}$ reduces to $\mathscr{A}_{N,n,+,0,z}=\cos^{-1}(0)=\pm\frac{\pi}{2}$. Due to the symmetry relation (Eq. 50), we deduce that the sign depends only on n and is given by $(-1)^{n+1}$. This completes the proof.

10.1002/cphc.202200951
WILEY-VCH

The Case $\theta = \frac{\pi}{2}$

By definition, we have Eq. 82:

$$\begin{cases} \psi_n(0) &= \begin{pmatrix} 0 \\ \sqrt{\frac{2}{N+2}} \sin\left(\frac{n\pi}{N+2}\right) \end{pmatrix} \\ \psi_n(N) &= \begin{pmatrix} 0 \\ \sqrt{\frac{2}{N+2}} \sin\left(\frac{n\pi(N+1)}{N+2}\right) \end{pmatrix} \end{cases} \tag{82}$$

As Eq. 83:

$$\begin{aligned} \sin\left(\frac{n\pi(N+1)}{N+2}\right) &= \sin\left(n\pi - \frac{n\pi}{N+2}\right) \\ &= (-1)^{n+1} \sin\left(\frac{n\pi}{N+2}\right) \end{aligned} \tag{83}$$

we obtain Eq. 84:

$$\psi_n(N) = (-1)^{n+1} \psi_n(0) \tag{84}$$

We deduce directly that for n odd, $\psi_n(N) = \psi_n(0)$ and the angle is null and for n even $\psi_n(N) = -\psi_n(0)$ and the angle is π. This concludes the proof.

Proof of the Formula for the OM Coefficients of C_2 Symmetry-Adapted Linear Combinations for $\theta = 0$ and $\theta = \frac{\pi}{2}$ Twisted Cumulene

The Case $\theta = \frac{\pi}{2}$

This is the simplest case. Indeed, denoting by $A_N(w)$ the $N \times N$ matrix given by Eq. 85:

$$A_N(w) = \begin{pmatrix} w & 1 & 0 & \dots & 0 \\ 1 & w & \ddots & \ddots & \vdots \\ 0 & \ddots & \ddots & \ddots & 0 \\ \vdots & & & & 1 \\ 0 & \dots 0 & & 1 & w \end{pmatrix}, \tag{85}$$

and posing as usual $w = \frac{\alpha - \lambda}{\beta}$, the secular determinant $S_N(\lambda)$ of the Hückel matrix H_N defined by $S_N(\lambda) = \det(H_N - \lambda\ \mathrm{Id})$ is such that (see Eq. 86):

$$S_N(\lambda) = \beta^N \left(P_N(w)\right)^2, \tag{86}$$

where $P_N(w) = \det(A_N(w))$ and A_N is the classical matrix associated with a N-linear chain of carbon atoms.

The N roots of S_N are doubly degenerate and are symmetrically distributed around the value α and are given by Eq. 87:

$$\lambda_n = \alpha + 2\beta \cos\left(k_{N,n}\right), \tag{87}$$

with $k_{N,n} = n\pi/N + 1$.

We refer to the work of C.A. Coulson (Ref. 33, Appendix p.393-394) for more details.

The Case $\theta = 0$

This case is more complicated. The secular determinant $S_N(\lambda)$ for the Hückel matrix reads in this case as Eq. 88:

$$S_N(\lambda) = \beta^N P_{N+1}(w) P_{N-1}(w) \tag{88}$$

We have $2N$ roots which are non-degenerate and obtained by intricating the symmetric roots of $P_{N+1}(w)$ and $P_{N-1}(w)$. The roots of P_{N-1} corresponding to the p_x system and those of P_{N+1} to the p_y system.

Symmetry-adapted linear combinations in C_2 of atomic orbitals coming from the p_x and p_y systems are possible only for atomic orbitals which are not too far in energy. As a consequence, we must understand how the two spectrums are intricated. Denoting by $\lambda_{n,y}$ the eigenvalues induced by the y part and $\lambda_{n,x}$ the eigenvalues induced by the x part we obtain an intrication of the form of Eq. 89:

$$\lambda_{N+1,y} < \lambda_{N-1,x} < \lambda_{N,y} < \dots < \lambda_{2,y} < \lambda_{1,x} < \lambda_{1,y}. \tag{89}$$

Taking explicit values (see just below), one can observe that taking n for a particular energy level corresponding to $\lambda_{n,y}$, $n = 2, \dots, N$, the closest values of $\lambda_{k,x}$ is obtained for $k = n - 1$.

As an example, taking $N = 3, 4$ and 5 representing only the value $2\cos(k_{N+1,n})$ for $\lambda_{n,y}$ and $2\cos(k_{N-1,n})$ for $\lambda_{n,x}$, we obtain:

- $N = 3$: $\lambda_{4,y} = \alpha + 1.618\beta < \lambda_{2,x} = \alpha + 1.000\beta < \lambda_{3,y} = \alpha + 0.618a < \lambda_{2,y} = \alpha - 0.618\beta < \lambda_{1,x} = \alpha - 1.000\beta < \lambda_{1,y} = \lambda_1 = \alpha - 1.618\beta$
- $N = 4$: $\lambda_{5,y} = \alpha + 1.732\beta < \lambda_{3,x} = \alpha + 1.414\beta < \lambda_{4,y} = \alpha + 1.000\beta < \lambda_{2,x} = \alpha + 0.000\beta < \lambda_{3,y} = \alpha + 0.0000\beta < \lambda_{2,y} = \alpha - 1.000\beta < \lambda_{1,x} = \alpha - 1.414\beta < \lambda_{1,y} = \alpha - 1.732\beta$
- $N = 5$: $\lambda_{6,y} = \alpha + 1.802\beta < \lambda_{4,x} = \alpha + 1.618\beta < \lambda_{5,y} = \alpha + 1.247\beta < \lambda_{3,x} = \alpha + 0.618\beta < \lambda_{4,y} = \alpha + 0.445\beta < \lambda_{3,y} = \alpha - 0.445\beta < \lambda_{2,x} = \alpha - 0.618\beta < \lambda_{2,y} = \alpha - 1.247 < \lambda_{1,x} = \alpha - 1.618\beta < \lambda_{1,y} = \alpha - 1.802\beta$

The intrication of these values is resumed in the following Figure 22 for each of these three cases:

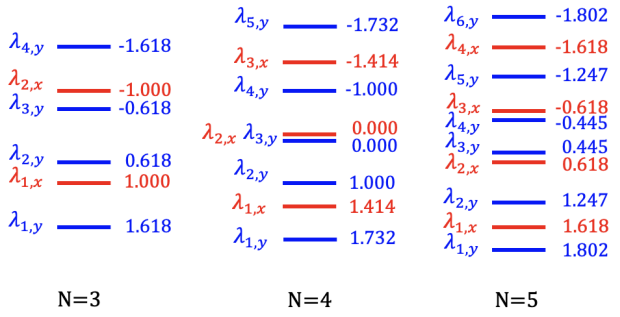

Figure 22. Representation in diagram form

As a consequence, taking the general form of the coefficients $c_{N,n}(z)$ for a linear chain given in Eq. 40, we obtain for a given N and $n = 2, \dots, N$ Eq. 90:

$$c^{\theta=0}_{y,n,N}(z) = c_{N+1,n}(z+1), \quad \text{and} \quad c^{\theta=0}_{x,n,N}(z) = c_{N-1,n-1}(z). \tag{90}$$

This concludes the proof. A working example is given in the next Section for $N = 3$ and $N = 4$.

10.1002/cphc.202200951
WILEY-VCH

Explicit Computations of C_2-Adapted Linear Combination of MOs for the $\theta = 0$ Twisted $[N]$-Cumulene, N =3, 4.

As an example of the computations and quantities manipulated in the previous section, we derive explicit values for the case $N = 3,4$ in the $\theta = 0$ case (see Figure 23), where the plane of the molecule is (z,x) and the orthogonal one corresponds to y.

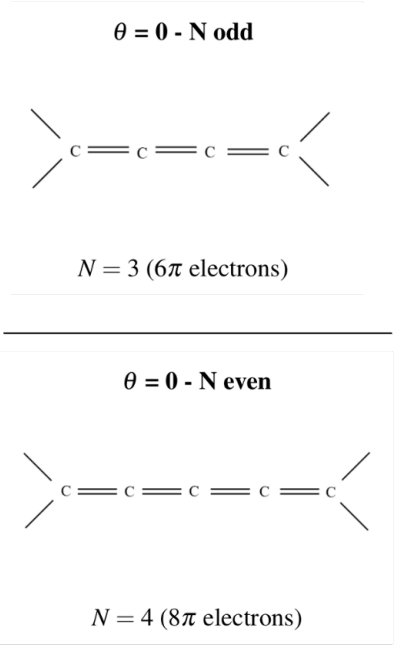

Figure 23. $N = 3,4$ cases of planar molecule

As already observed, the molecular orbitals are made of two perpendicular π systems contained in the (x,z) plane and (z,y) plane respectively corresponding to a $N+1$ linear chain in the (z,y) plane represented in blue and a $N-1$ linear chain in the (x,z) plane (see Figures 24 and 25).

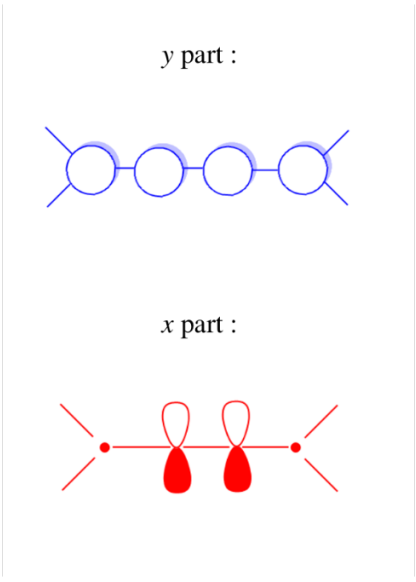

Figure 24. π systems for $N = 3$ case

The coefficients $c^{\theta=0}_{y,N,n}(z)$ computed for all values of n and z using formula and finally the corresponding eigenvalues corresponding to $2\cos(\frac{\pi n}{N+2})$ Eq. 90 are reported in Tables 3 and 4.

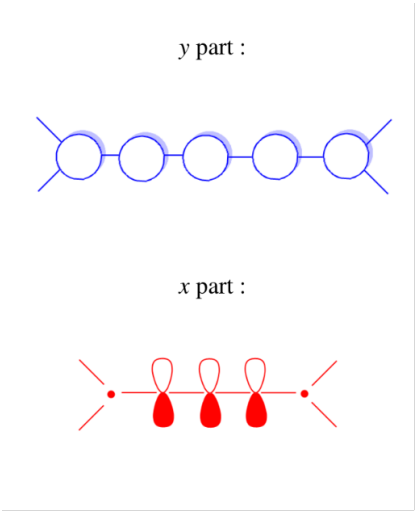

Figure 25. π systems for $N = 4$ case

Table 3. $c^{\Theta=0}_{y,3,n}(z)$ coefficients

z/n	1	2	3	4
0	0.370	0.600	0.600	0.370
1	0.600	0.370	-0.370	-0.600
2	0.600	-0.370	-0.370	0.600
3	0.370	-0.600	0.600	-0.370
$\lambda_{n,y}$	1.618	0.618	-0.618	-1.618

Table 4. $c^{\Theta=0}_{y,4,n}(z)$ coefficients

z/n	1	2	3	4	5
0	0.289	0.500	0.577	0.500	0.289
1	0.500	0.500	0.000	-0.500	-0.500
2	0.577	0.000	-0.577	0.000	0.577
3	0.500	-0.500	0.000	0.500	-0.500
4	0.289	-0.500	0.577	-0.500	0.289
$\lambda_{n,y}$	1.732	1.000	0.000	-1.000	-1.732

These values corresponding for each n to the MOs configurations are depicted in Figure 26.

In the same way, the coefficients $c^{\theta=0}_{x,N,n}(z)$ are given in Tables 5 and 6

The MOs configurations obtained for each n are shown in Figure 27.

We then report in Tables 7 and 8 the C_2-adapted linear combinations of MOs using equation Eq. 47.

Supporting Information Summary

Additional references cited within the Supporting Information [34–36]. Supporting Information highlights more details on results obtained for different cases: cumulenes, diphenylbutadiene, tolanophane and metallacumulene.

10.1002/cphc.202200951
WILEY-VCH

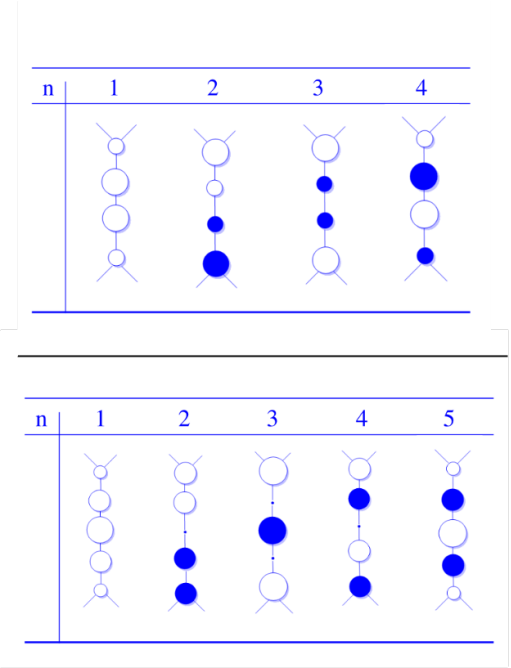

Figure 26. Projections of y-values for MOs configurations for $N = 3,4$ cases.

Table 5. $c^{\Theta=0}_{x,3,n}(z)$ coefficients

z/n	1	2	3	4
0	-	0.000	0.000	-
1	-	0.707	0.707	-
2	-	0.707	-0.707	-
3	-	0.000	0.000	-
$\lambda_{n,x}$	-	1.000	-1.000	-

Table 6. $c^{\Theta=0}_{x,4,n}(z)$ coefficients

z/n	1	2	3	4	5
0	-	0.000	0.000	0.000	-
1	-	0.500	0.707	0.500	-
2	-	0.707	0.000	-0.707	-
3	-	0.500	-0.707	0.500	-
4	-	0.000	0.000	0.000	-
$\lambda_{n,x}$	-	1.414	0.000	-1.414	-

Acknowledgements

The project leading to this publication has received funding from Excellence Initiative of Université de Pau et des Pays de l'Adour - I-Site E2S UPPA, a French "Investissement d'Avenir" program. This article was also supported by the Défi CNRS "Biomimétisme" in collaboration with the Université Claude Bernard Lyon 1 and Université de Lyon. We would also like to thank Professor C. Wentrup for discussions on cumulenes, and Dr G. Salvato-Vallverdu for VASP calculations and discussions.

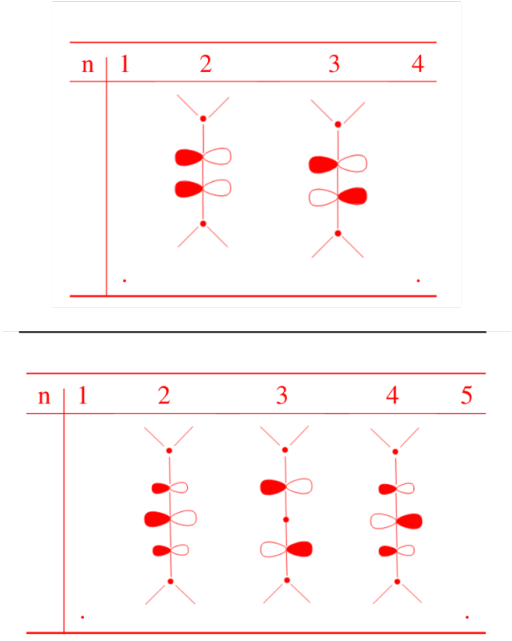

Figure 27. Projections of x-values for MOs configurations for $N = 3,4$ cases.

Table 7. $\Psi_{3,n}(z)$ C_2-adapted linear combinations of MOs

z/n	2	3
0	$\begin{pmatrix}0.000\\0.600\end{pmatrix}$	$\begin{pmatrix}0.000\\0.600\end{pmatrix}$
1	$\begin{pmatrix}0.707\\0.370\end{pmatrix}$	$\begin{pmatrix}0.707\\-0.370\end{pmatrix}$
2	$\begin{pmatrix}0.707\\-0.370\end{pmatrix}$	$\begin{pmatrix}-0.707\\-0.370\end{pmatrix}$
3	$\begin{pmatrix}0.000\\-0.600\end{pmatrix}$	$\begin{pmatrix}0.000\\0.600\end{pmatrix}$

Table 8. $\Psi_{4,n}(z)$ C_2-adapted linear combinations of MOs

z/n	1	2	3	4	5
1	$\begin{pmatrix}0.000\\0.289\end{pmatrix}$	$\begin{pmatrix}0.000\\0.500\end{pmatrix}$	$\begin{pmatrix}0.000\\0.577\end{pmatrix}$	$\begin{pmatrix}0.000\\0.500\end{pmatrix}$	$\begin{pmatrix}0.000\\0.289\end{pmatrix}$
2	$\begin{pmatrix}0.000\\0.500\end{pmatrix}$	$\begin{pmatrix}0.500\\0.500\end{pmatrix}$	$\begin{pmatrix}0.707\\0.000\end{pmatrix}$	$\begin{pmatrix}0.500\\-0.500\end{pmatrix}$	$\begin{pmatrix}0.000\\-0.500\end{pmatrix}$
3	$\begin{pmatrix}0.000\\0.577\end{pmatrix}$	$\begin{pmatrix}0.707\\0.000\end{pmatrix}$	$\begin{pmatrix}0.000\\-0.577\end{pmatrix}$	$\begin{pmatrix}-0.707\\0.000\end{pmatrix}$	$\begin{pmatrix}0.000\\0.577\end{pmatrix}$
4	$\begin{pmatrix}0.000\\0.500\end{pmatrix}$	$\begin{pmatrix}0.500\\-0.500\end{pmatrix}$	$\begin{pmatrix}-0.707\\0.000\end{pmatrix}$	$\begin{pmatrix}0.500\\0.500\end{pmatrix}$	$\begin{pmatrix}0.000\\-0.500\end{pmatrix}$
5	$\begin{pmatrix}0.000\\0.289\end{pmatrix}$	$\begin{pmatrix}0.000\\-0.500\end{pmatrix}$	$\begin{pmatrix}0.000\\0.577\end{pmatrix}$	$\begin{pmatrix}0.000\\-0.500\end{pmatrix}$	$\begin{pmatrix}0.000\\0.289\end{pmatrix}$

Conflict of Interest

Please enter any conflict of interest to declare.

Keywords: chirality • Curie's principle • helical orbitals •

linear chains • mathematical concepts

References

[1] M. H. Garner, R. Hoffmann, S. Rettrup, G. C. Solomon, *ACS Cent. Sci.* **2018**, *4*, 688.
[2] C. H. Hendon, D. Tiana, A. T. Murray, D. R. Carbery, A. Walsh, *Chem. Sci.* **2013**, *4*, 4278.
[3] A. Imamura, Y. Aoki, *Chem. Phys. Lett.* **2013**, *590*, 136.
[4] Y. Aoki, O. Yuuichi, A. Imamura, *ACS Central Science* **2018**, *4*, 664.
[5] P. Sarbadhikary, S. Shil, A. Panda, A. Misra, *J. Org. Chem.* **2016**, *81*, 5623.
[6] J. B. G. Gluyas, S. Gückel, M. Kaupp, P. J. Low, *Chem. Eur. J.* **2016**, *22*, 16138.
[7] M. D. Peeks, P. Neuhaus, H. L. Anderson, *Phys. Chem. Chem. Phys* **2016**, *18*, 5264.
[8] W. R. Martin, D. W. Ball, *ChemistrySelect* **2018**, *3*, 7222.
[9] P. Baronas, R. Komskis, E. Tankelevičiu̅tė, P. Adomėnas, O. Adomėnienė, S. Juršėnas, *J. Phys. Chem. Lett.* **2021**, *12*, 6827.
[10] W. Bro-Jørgensen, M. H. Garner, G. C. Solomon, *J. Phys. Chem. A* **2021**, *125*, 8107.
[11] S. Gunasekaran, L. Venkataraman, *J. Chem. Phys.* **2020**, *153*, 124304.
[12] P. Pinter, D. Munz, *J. Phys. Chem. A.* **2020**, *124*, 10100.
[13] Y. Orimoto, Y. Aoki, A. Imamura, *J. Phys. Chem. C.* **2019**, *123*, 11134.
[14] O. Cretu, H.-P. Komsa, O. Lehtinen, G. Algara-Siller, U. Kaiser, K. Suenaga, A. Krasheninnikov, *ACS Nano* **2014**, *8*, 11950.
[15] P. O. Löwdin, *J. Math. Phys.* **1962**, *3*, 969.
[16] L. Jin, Z. Song, *Phys. Rev. A* **2011**, *83*, 062118.
[17] P. Curie, *J. Phys. Theor. Appl.* **1894**, *3*, 393.
[18] A. F. Chalmers, *Brit. J. Phil. Sci.* **1970**, *21*, 133.
[19] J. Ismael, *Synthese* **1997**, *110*, 167.
[20] M. Rérat, B. Kirtman, *J. Chem. Theory Comput.* **2021**, *17*, 4063.
[21] J. Escudié, H. Ranaivonjatovo, L. Rigon, *Chem. Rev.* **2000**, *100*, 3639.
[22] G. Cavigliasso, N. Kaltsoyannis, *Inorg. Chem.* **2006**, *45*, 6828.
[23] A. Burgun, F. Gendron, C. J. Sumby, T. Roisnel, O. Cador, K. Costuas, J.-F. Halet, M. I. Bruce, C. Lapinte, *Organometallics* **2014**, *33*, 2613.
[24] M. Akita, T. Koike, *Dalton Trans.* **2008**, pages 3523–3530.
[25] F. Gendron, *Theoretical Study of Inorganic Molecular Systems: From Molecules to Devices, PhD Thesis*, Ph.D. thesis, University of Rennes 1, France **2012**.
[26] S. Huang, X. Hong, H.-Z. Cui, B. Zhan, Z.-M. Li, X.-F. Hou, *Organometallics* **2020**, *39*, 3514.
[27] M. J. Frisch, G. W. Trucks, H. B. Schlegel, G. E. Scuseria, M. A. Robb, J. R. Cheeseman, G. Scalmani, G. A. Barone, V. Petersson, H. Nakatsuji, X. Li, M. Caricato, A. Marenich, J. Bloino, B. G. Janesko, R. Gomperts, B. Mennucci, H. P. Hratchian, J. V. Ortiz, A. F. Izmaylov, J. L. Sonnenberg, D. Williams-Young, F. Ding, F. Lipparini, F. Egidi, J. Goings, B. Peng, A. Petrone, T. Henderson, D. Ranasinghe, V. G. Zakrzewski, J. Gao, N. Rega, G. Zheng, W. Liang, M. Hada, M. Ehara, K. Toyota, R. Fukuda, J. Hasegawa, M. Ishida, T. Nakajima, Y. Honda, O. Kitao, H. Nakai, T. Vreven, K. Throssell, J. A. Montgomery, J. J. Peralta, E. F. Ogliaro, M. Bearpark, J. J. Heyd, E. Brothers, K. N. Kudin, V. N. Staroverov, T. Keith, R. Kobayashi, J. Normand, K. Raghavachari, A. Rendell, J. C. Burant, S. S. Iyengar, J. Tomasi, M. Cossi, J. M. Millam, M. Klene, C. Adamo, R. Cammi, J. W. Ochterski, R. L. Martin, K. Morokuma, O. Farkas, J. B. Foresman, D. J. Fox, Gaussian 09, Revision A.2 **2009**, Gaussian. Inc.: Wallingford. CT.
[28] H.-J. Werner, P. J. Knowles, G. Knizia, F. R. Manby, M. Schütz, P. Celani, W. Györffy, D. Kats, T. Korona, R. Lindh, A. Mitrushenkov, G. Rauhut, K. R. Shamasundar, T. B. Adler, R. D. Amos, A. Bernhardsson, A. Berning, D. L. Cooper, M. J. O. Deegan, A. J. Dobbyn, F. Eckert, E. Goll, C. Hampel, A. Hesselmann, G. Hetzer, T. Hrenar, G. Jansen, C. Köppl, Y. Liu, A. W. Lloyd, R. A. Mata, A. J. May, S. J. McNicholas, W. Meyer, M. E. Mura, A. Nicklass, D. P. O'Neill, P. Palmieri, D. Peng, K. Pflüger, R. Pitzer, M. Reiher, T. Shiozaki, H. Stoll, A. J. Stone, R. Tarroni, T. Thorsteinsson, M. Wang, MOLPRO, version 2015.1, a package of *ab initio* programs **2015**, see "http://www.molpro.net".
[29] G. Kresse, J. Furthmüller, *Comput. Mater. Sci.* **1996**, *6*, 15.
[30] G. Kresse, J. Furthmüller, *Phys. Rev. B* **1996**, *54*, 11169.
[31] G. Kresse, D. Joubert, *Phys. Rev. B* **1999**, *59*, 1758.
[32] A. E. Reed, F. Weinhold, *J. Chem. Phys.* **1985**, *83*, 1736.
[33] C. A. Coulson, *Proc. R. Soc. A.* **1938**, *164*, 383.
[34] S. Toyota, K. Kawai, T. Iwanaga, K. Wakamatsu, *Eur. J. Org. Chem.* **2012**, *2012*, 5679.
[35] M. Liu, V. I. Artyukhov, H. Lee, F. Xu, B. I. Yakobson, *ACS Nano* **2013**, *7*, 10075.
[36] A. Ozcelik, D. Aranda, S. Gil-Guerrero, X. A. Pola-Otera, M. Talavera, L. Wang, S. Kumar Behera, J. Gierschner, A. Pena-Gallego, F. Santoro, R. Pereira-Cameselle, J. Lorenzo Alonso-Gomez, *Chem. Eur. J.* **2020**, *26*, 17342.

10.1002/cphc.202200951
WILEY-VCH

Entry for the Table of Contents

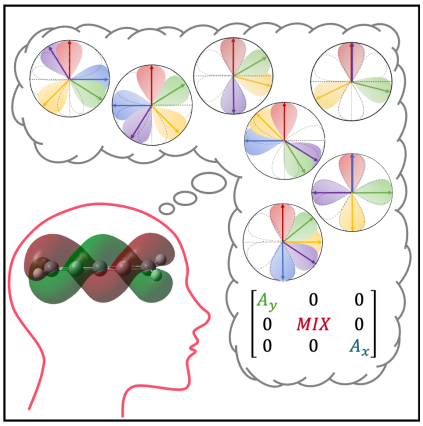

We deeply detail mathematical concepts behind the generation of helical molecular orbitals (MOs) for linear chains of atoms. After defining helical MOs, we provide an index measuring how far a given helical states is from a perfect helical distribution. Structural properties of helical distribution for twisted cumulene version of Möbius systems are also discussed. Furthermore, some structural assumptions as well as symmetry requirements ensuring the existence of helical MOs are given.

Twitter Handles

- Universite de Pau et des Pays de l'Adour: @universite_uppa
- I-Site E2S UPPA: @E2sUppa
- IPREM: @UMR5254
- ISCR: @chimie_ISCR
- CTI-ISCR team: @theochem_ISCR